Supporting Information for:

Dynamic helical poly[4]helicene nanoribbon

Tomoyuki Ikai,[1,2,*] Hayato Inagaki,[1] Kosuke Oki,[1,3] Masaya Yoshida,[1] Jenny Pirillo,[4] Yuh Hijikata,[5] and Eiji Yashima[1,6,*]

[1] Department of Molecular and Macromolecular Chemistry, Graduate School of Engineering, Nagoya University, Chikusa-ku, Nagoya 464-8603, Japan

[2] Precursory Research for Embryonic Science and Technology (PRESTO), Japan Science and Technology Agency (JST), Kawaguchi, Saitama 332-0012, Japan

[3] Present address: Faculty of Science and Technology, Seikei University, Musashino, Tokyo 180-8633, Japan

[4] Department of Materials Chemistry, Graduate School of Engineering, Nagoya University, Chikusa-ku, Nagoya 464-8603, Japan

[5] Research Center for Net Zero Carbon Society, Institute of Innovation for Future Society, Nagoya University, Chikusa-ku, Nagoya 464-8601, Japan

[6] Present address: Department of Chemical Engineering, National Tsing Hua University, 101, Sec. 2, Kuang-Fu Road, Hsinchu, 30013, Taiwan, R.O.C.

* Correspondence: ikai@chembio.nagoya-u.ac.jp; yashima@chembio.nagoya-u.ac.jp

Table of Contents

1. Instruments and Materials

Instruments. The melting points were measured on a Yanako melting point apparatus (Yanako, Kyoto, Japan) and were uncorrected. The NMR spectra were measured using a Varian 500AS (Agilent Technologies, Santa Clara, CA) or a Bruker Ascend 500 (Bruker Biospin, Billerica, MA) spectrometer operating at 500 MHz for ^{1}H and 126 MHz for ^{13}C using tetramethylsilane or a solvent residual peak as the internal standard. The IR spectra were recorded on a JASCO FT/IR-6X spectrophotometer (JASCO, Tokyo, Japan) equipped with a JASCO ATR PRO ONE X attenuated total reflectance attachment (ZnSe prism). The absorption and circular dichroism (CD) spectra were obtained in a 1.0- or 10-mm quartz cell using a JASCO V-750 spectrophotometer and a JASCO J-1500 spectropolarimeter, respectively. The concentrations of the polymers were calculated based on the monomer units. The temperature was controlled with a JASCO ETCS-900 apparatus. The photoluminescence (PL) and circularly polarized luminescence (CPL) spectra were recorded at 25 °C on a JASCO CPL-300 spectrophotometer with a 1.0-mm quartz cell. A scanning rate of 200 nm/min, an excitation slit width of 3000 μm, a monitoring slit width of 3000 μm, a response time of 2 seconds, and 32 times accumulations were employed for the CPL measurements. Fluorescence quantum yields were measured with a JASCO FP-8550 spectrofluorometer attached with a JASCO ILF-135 integrating sphere (diameter 120 mm). The size exclusion chromatography (SEC) measurements were performed with a JASCO PU-4580 liquid chromatograph equipped with a JASCO CO-4060 column oven and a JASCO MD-2018 multi-wavelength UV/VIS detector. The number-average molar mass (M_n) and its dispersity (M_w/M_n) were determined at 40 °C using a Tosoh TSKgel GMH$_{HR}$-M (30 cm × 7.8 mm (i.d.)) SEC column (Tosoh, Tokyo, Japan), and chloroform was used as the eluent at a flow rate of 1.0 mL/min. The molar mass calibration curve was obtained with polystyrene standards (Tosoh). Recycling preparative high-performance liquid chromatography (HPLC) was performed with a JAI LC-7080 liquid chromatograph (JAI, Tokyo, Japan) equipped with a JAI UV-800LA UV detector at room temperature. JAIGEL-1HR and JAIGEL-2HR (60 cm × 2.0 cm (i.d.)) connected in series were used as columns (JAI), and chloroform was used as the eluent at a flow rate of 9.0 mL/min. The removal of low-molar-mass oligomers from an as-synthesized precursor polymer was performed using HPLC equipped with a JASCO PU-4185 Binary HPLC pump and a JASCO MD-2018 multi-wavelength UV/VIS detector, and a Tosoh TSKgel GMHXL (30 cm × 21.5 mm (i.d.)) was used as a column. The high-resolution mass spectra (HRMS) were recorded on a Bruker compact QTOF (Bruker Daltonics, Billerica, MA) spectrometer with atmospheric pressure chemical ionization (APCI). The matrix-assisted laser desorption-ionization time-of-flight mass (MALDI-TOF-MS) spectra were measured on a Bruker ultrafleXtreme TOF/TOF mass spectrometer (Bruker Daltonics, Bremen, Germany) using *trans*-2-[3-(4-*tert*-butylphenyl)-2-methyl-2-propenylidene]malononitrile as the ionizing matrix. The single crystal X-ray diffraction measurements were performed on a Rigaku Saturn 724+ CCD diffractometer (Rigaku, Tokyo, Japan) with Mo Kα radiation (λ = 0.71073 Å) at 93 K.

Materials. All starting materials and anhydrous solvents were purchased from Sigma-Aldrich (St. Louis, MO), Fujifilm Wako Pure Chemical (Osaka, Japan), Tokyo Kasei (TCI, Tokyo, Japan), or Kanto Kagaku (Tokyo, Japan) and were used as received. Bis[2-(4-alkoxy-2,6-dimethylphenyl)ethynyl]phenylene compounds (**7**[S1] and **Ph$_{Br}$**[S2]) and 1,5-bis(4,4,5,5-tetramethyl-1,3,2-dioxaborolan-2-yl)naphthalene (**NAP$_{Bpin}$**)[S3] were synthesized according to the previously reported methods.

2. Synthetic Procedures

Consecutively fused multiple [4]helicenes (double-**2** and quadruple-**4**) were prepared according to Supplementary Scheme 1.

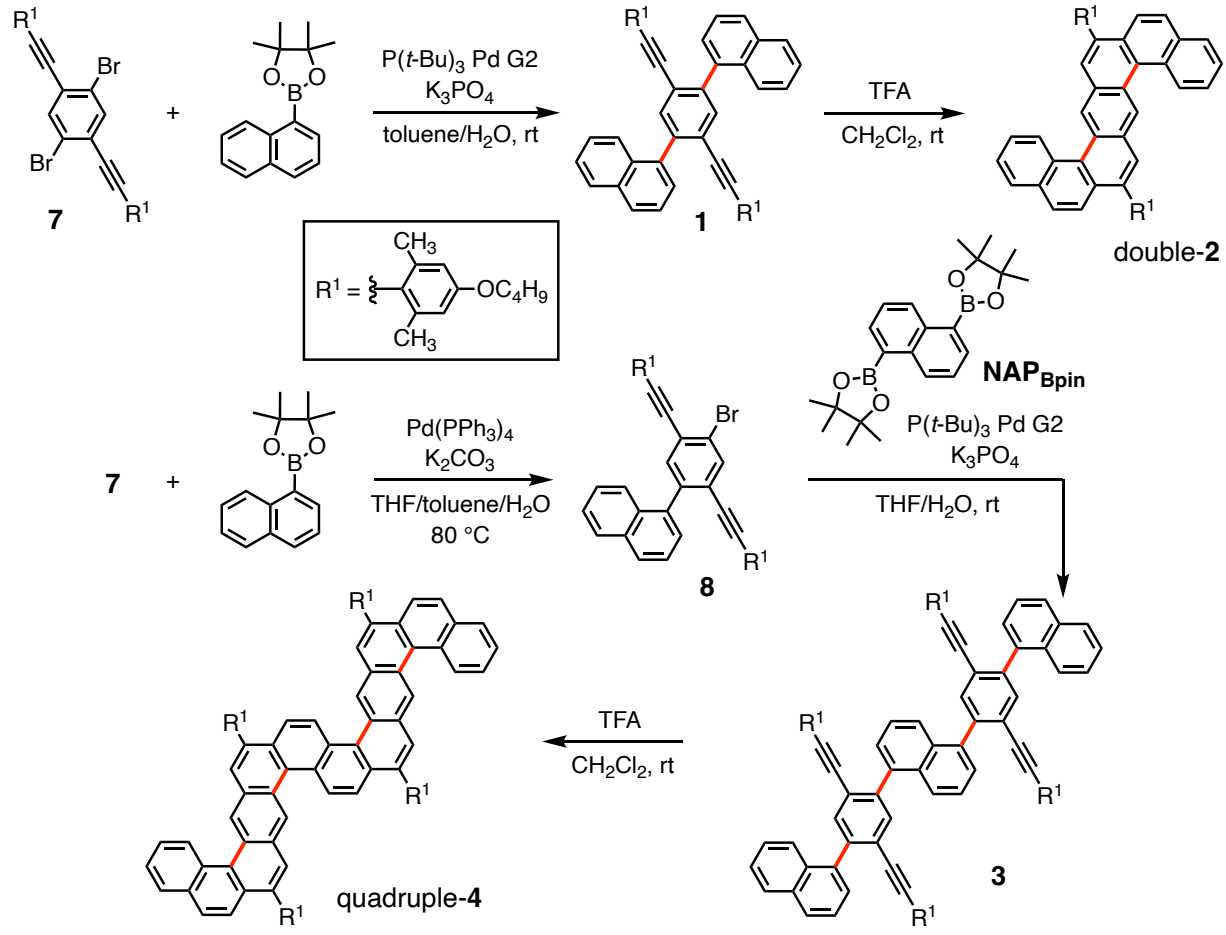

Supplementary Scheme 1 | Synthesis of double-**2** and quadruple-**4**.

Synthesis of 1. To a mixture of **7** (60 mg, 0.095 mmol), 4,4,5,5-tetramethyl-2-(naphthalen-1-yl)-1,3,2-dioxaborolane (55 mg, 0.22 mmol), and tripotassium phosphate (0.10 g, 0.47 mmol) in a degassed toluene/water mixture (5/2, v/v; 2.1 mL) was added chloro[(tri-*tert*-butylphosphine)-2-(2-aminobiphenyl)]palladium(II) (P(*t*-Bu)$_3$ Pd G2) (5.4 mg, 10 μmol). After stirring at room temperature for 4 h, the mixture was diluted with chloroform and the solution was washed with water, and then dried over Na_2SO_4. The solvents were removed under reduced pressure and the residue was passed through a short pad of silica gel using *n*-hexane/ethyl acetate (7/3, v/v) as the eluent. After concentrating in vacuo, the crude product was purified by recycling preparative HPLC on JAIGEL-1H and JAIGEL-2H (60 cm × 2.0 cm (i.d.)) using chloroform as the eluent to give the desired product as a pale yellow solid (25 mg, 36% yield). Mp: 238.9–239.4 °C. IR (ATR, cm^{-1}): 2201 (C≡C). ^{1}H NMR (500 MHz, 1,1,2,2-tetrachloroethane-d_2, 95 °C): δ 7.98-7.96 (m, 4H, Ar–H), 7.95-7.88 (br, 2H, Ar–H), 7.77 (s, 2H, Ar–H), 7.72-7.67 (br, 2H, Ar–H), 7.65-7.62 (m, 2H, Ar–H), 7.57-7.54 (m, 4H, Ar–H), 6.44 (s, 4H, Ar–H), 3.91 (t, J = 6.6 Hz, 4H, OCH_2), 1.82 (s, 12H, Ar–CH_3), 1.76-1.70 (m, 4H, CH_2), 1.52-1.44 (m, 4H, CH_2), 0.99 (t, J = 7.5 Hz, 6H, CH_3). ^{13}C NMR (126 MHz, 1,1,2,2-tetrachloroethane-d_2, 95 °C): δ 158.72, 141.88, 141.19, 138.50, 133.78, 133.66, 132.18, 127.90, 127.80, 127.11, 126.23, 125.94, 125.60, 125.19, 123.88, 115.05, 113.06, 95.55, 92.24, 67.66, 31.16, 20.21, 18.94, 13.38. HRMS (APCI+): *m*/*z* calcd for $C_{54}H_{51}O_2$ ($M+H^+$), 731.3884; found 731.3895.

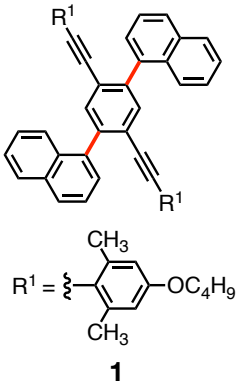

1

Synthesis of double-2. **1** (9.8 mg, 13 μmol) was dissolved in an anhydrous dichloromethane/trifluoroacetic acid (TFA) mixture (60/1, v/v; 2.0 mL) and the solution was stirred at room temperature for 1 h. After quenching the reaction with saturated aqueous $NaHCO_3$, the mixture was diluted with chloroform and the solution was washed with saturated aqueous $NaHCO_3$ and water, and then dried over Na_2SO_4. The solvents were removed under reduced pressure and the product was passed through a short pad of silica gel using chloroform as the eluent to give the desired product as a yellow solid (9.6 mg, 98% yield). Mp: decomposed at >200 °C. ^{1}H NMR (500 MHz, $CDCl_3$, 25 °C): δ 9.66 (s, 2H, Ar–H), 9.42 (d, J = 8.5 Hz, 2H, Ar–H), 8.05 (d, J = 8.1 Hz, 2H, Ar–H), 7.92 (s, 2H, Ar–H), 7.85 (d, J = 8.8 Hz, 2H, Ar–H), 7.78-7.75 (m, 2H, Ar–H), 7.68-7.65 (m, 2H, Ar–H), 7.49 (d, J = 8.5 Hz, 2H, Ar–H), 6.80 (s, 4H, Ar–H), 4.07 (t, J = 6.5 Hz, 4H, OCH_2), 2.00 (s, 12H, Ar–CH_3), 1.87-1.82 (m, 4H, CH_2), 1.61-1.55 (m, 4H, CH_2), 1.04 (t, J = 7.3 Hz, 6H, CH_3). ^{13}C NMR (126 MHz, $CDCl_3$, rt): δ 158.35, 138.55, 137.20, 133.28, 131.97, 131.45, 130.67, 130.61, 128.87, 128.48, 128.43, 127.97, 127.84, 127.74, 127.68, 126.48, 125.94, 124.01, 113.30, 67.57, 31.52, 20.92, 19.36, 13.95. HRMS (APCI+): *m*/*z* calcd for $C_{54}H_{51}O_2$ ($M+H^+$), 731.3884; found 731.3885.

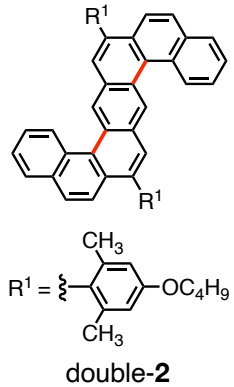

double-**2**

Synthesis of 8. To a mixture of **7** (500 mg, 0.786 mmol), 4,4,5,5-tetramethyl-2-(naphthalen-1-yl)-1,3,2-dioxaborolane (309 mg, 1.22 mmol), and potassium carbonate (138 mg, 2.05 mmol) in a degassed tetrahydrofuran (THF)/toluene/water mixture (8/5/2, v/v; 15 mL) was added tetrakis(triphenylphosphine)palladium(0) ($Pd(PPh_3)_4$) (101 mg, 87.4 μmol). After stirring at 80 °C for 45 h, the mixture was diluted with chloroform and the solution was washed with water, and then dried over Na_2SO_4. The solvents were removed under reduced pressure and the residue was passed through a short pad of silica gel using *n*-hexane/ethyl acetate (99/1, v/v) as the eluent. After concentrating in vacuo, the crude product was purified by recycling preparative HPLC on JAIGEL-1H and JAIGEL-2H (60 cm × 2.0 cm (i.d.)) using chloroform as the eluent to give the desired product as a pale yellow solid (298 mg, 55% yield).

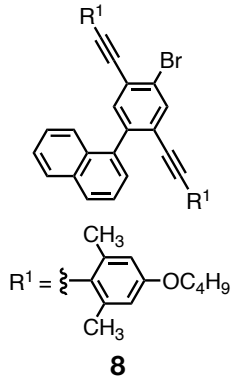

8

Mp: 117.1–117.5 °C. ^{1}H NMR (500 MHz, $CDCl_3$, 25 °C): δ 7.90 (s, 1H, Ar–H), 7.88 (d, J = 8.1 Hz, 2H, Ar–H), 7.65 (d, J = 8.3 Hz, 1H, Ar–H), 7.54-7.51 (m, 2H, Ar–H), 7.48-7.45 (m, 2H, Ar–H), 7.43-7.40 (m, 1H, Ar–H), 6.61 (s, 2H, Ar–H), 6.37 (s, 2H, Ar–H), 3.95 (t, J = 6.5 Hz, 2H, OCH_2), 3.83 (t, J = 6.5 Hz, 2H, OCH_2), 2.51 (s, 6H, Ar–CH_3), 1.78-1.64 (m, 10H, Ar–CH_3, CH_2), 1.52-1.39 (m, 4H, CH_2), 0.97 (t, J = 7.4 Hz, 3H, CH_3), 0.92 (t, J = 7.4 Hz, 3H, CH_3). ^{13}C NMR (126 MHz, $CDCl_3$, rt): δ 159.13, 158.82, 142.65, 142.22, 141.10, 137.64, 135.01, 134.45, 133.63, 131.81, 128.18, 128.05, 126.89, 126.26, 126.08, 125.89, 125.37, 125.24, 123.28, 114.62, 114.42, 113.04, 112.67, 94.83, 94.27, 93.98, 93.19, 67.54, 67.41, 31.27, 31.19, 21.60, 20.45, 19.23, 19.16, 13.85, 13.80.

Synthesis of 3. To a mixture of **8** (79 mg, 0.12 mmol), **NAP$_{Bpin}$** (21 mg, 0.054 mmol), and tripotassium phosphate (56 mg, 0.26 mmol) in a degassed THF/water mixture (2/1, v/v; 0.90 mL) was added P(*t*-Bu)$_3$ Pd G2 (3.7 mg, 7.2 μmol). After stirring at room temperature for 7 h, the mixture was diluted with chloroform and the solution was washed with water, and then dried over Na_2SO_4. The solvent was removed under reduced pressure and the crude product was purified by silica gel chromatography using *n*-hexane/chloroform (9/1, v/v) as the eluent to give the desired product as a pale yellow solid (60 mg, 83% yield).

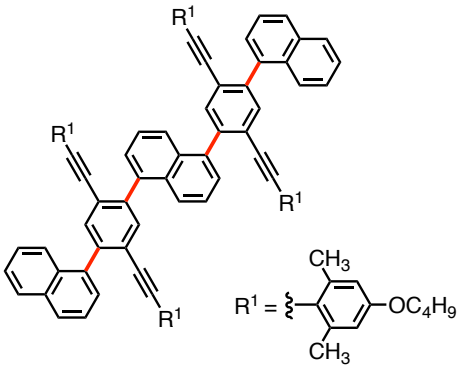

3

Mp: decomposed at >240 °C. IR (ATR, cm^{-1}): 2202 (C≡C). ^{1}H NMR (500 MHz, 1,1,2,2-tetrachloroethane-d_2, 95 °C): δ 8.10-7.88 (br, 8H, Ar–H), 7.88-7.78 (br, 4H, Ar–H), 7.78-7.62 (br, 8H, Ar–H), 7.62-7.50 (br, 4H, Ar–H), 6.50-6.40 (br, 7H, Ar–H), 6.24-6.15 (br, 1H, Ar–H), 3.91 (t, J = 6.4 Hz, 7H, OCH_2), 3.80-3.68 (br, 1H, OCH_2), 1.94-1.80 (br, 24H, CH_3), 1.76-1.71 (m, 8H, CH_2), 1.52-1.45 (m, 8H, CH_2), 1.01-0.97 (m, 12H, CH_3). ^{13}C NMR (126 MHz, 1,1,2,2-tetrachloroethane-

d_2, 95 °C): δ158.76, 141.85, 141.60, 141.20, 138.59, 138.52, 133.81, 133.73, 132.48, 132.20, 127.94, 127.84, 127.16, 126.25, 125.99, 125.63, 125.45, 125.22, 124.00, 123.86, 115.07, 113.10, 95.69, 92.23, 67.67, 31.17, 20.35, 20.26, 18.95, 13.41, 13.39. HRMS (APCI+): *m*/*z* calcd for $C_{98}H_{93}O_4$ ($M+H^+$), 1333.7068; found 1333.7038.

Synthesis of quadruple-4. **3** (9.0 mg, 6.7 μmol) was dissolved in an anhydrous dichloromethane/TFA mixture (60/1, v/v; 1.0 mL) and the solution was stirred at room temperature for 1 h. After quenching the reaction with saturated aqueous $NaHCO_3$, the mixture was diluted with chloroform and the solution was washed with saturated aqueous $NaHCO_3$ and water, and then dried over Na_2SO_4. The solvents were removed under reduced pressure and the product was passed through a short pad of silica gel using chloroform as the eluent to give the desired product as a yellow solid (8.8 mg, 98% yield). Mp: decomposed at >210 °C. ^{1}H NMR (500 MHz, $CDCl_3$, 25 °C): δ9.70 (s, 2H, Ar–H), 9.59 (s, 2H, Ar–H), 9.46 (d, J = 8.5 Hz, 2H, Ar–H), 9.39 (d, J = 9.0 Hz, 2H, Ar–H), 8.06 (d, J = 8.3 Hz, 2H, Ar–H), 7.99 (s, 2H, Ar–H), 7.88 (s, 2H, Ar–H), 7.85 (d, J = 8.8 Hz, 2H, Ar–H), 7.80-7.77 (m, 2H, Ar–H), 7.68-7.66 (m, 4H, Ar–H), 7.49 (d, J = 8.8 Hz, 2H, Ar–H), 6.82 (s, 4H, Ar–H), 6.77 (s, 4H, Ar–H), 4.08-4.03 (m, 8H, OCH_2), 2.09 (s, 12H, Ar–CH_3), 1.98 (s, 12H, Ar–CH_3), 1.87-1.80 (m, 8H, CH_2), 1.60-1.55 (m, 8H, CH_2), 1.04-1.01 (m, 12H, CH_3). ^{13}C NMR (126 MHz, $CDCl_3$, rt): δ158.43, 158.34, 138.59, 138.50, 137.25, 136.91, 133.33, 131.97, 131.95, 131.53, 130.95, 130.73, 130.69, 130.22, 129.08, 128.89, 128.62, 128.51, 128.38, 128.19, 128.00, 127.95, 127.88, 127.78, 127.73, 126.50, 125.94, 124.02, 113.40, 113.32, 67.59, 31.53, 21.02, 20.87, 19.37, 13.93. HRMS (APCI+): *m*/*z* calcd for $C_{98}H_{93}O_4$ ($M+H^+$), 1333.7068; found 1333.7069.

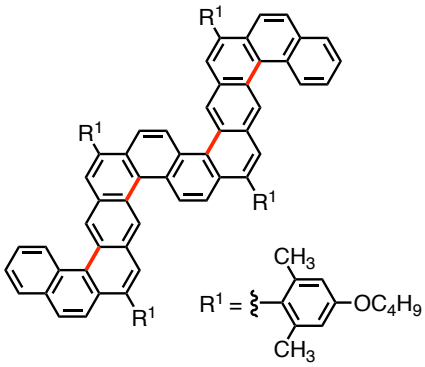

quadruple-**4**

Polymerization. Suzuki–Miyaura coupling copolymerizations of the diboronic acid bis(pinacol) ester (**Ph$_{Br}$**) with **NAP$_{Bpin}$** were carried out according to Supplementary Scheme 2 in a dry Schlenk flask under a dry nitrogen atmosphere using P(*t*-Bu)$_3$ Pd G2 as a catalyst in a similar way as reported previously.[S2] The results of the copolymerizations are summarized in Supplementary Table 1. The M_n and M_w/M_n values of the random-coil precursor polymers were estimated by SEC using polystyrene standards in chloroform.

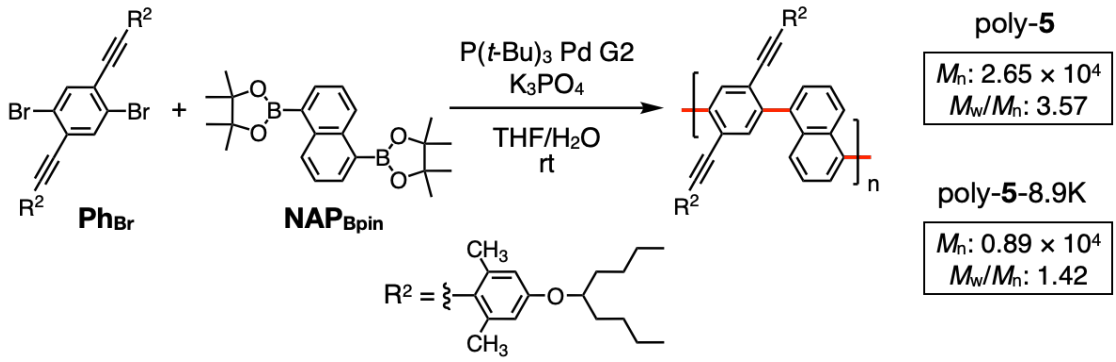

Supplementary Scheme 2 | Synthesis of poly-**5** and poly-**5**-8.9K.

Supplementary Table 1. Copolymerization Results of Ph$_{Br}$ with NAP$_{Bpin}$ Using P(*t*-Bu)$_3$ Pd G2 in the Presence of K$_3$PO$_4$ in THF/H$_2$O (2/1, v/v) at Room Temperature.[a]

entry	monomer in feed (mol%)		reaction time	copolymer				
				sample code	yield (%) [b]	M_n (10^4) [c]	M_w/M_n [c]	DP_n [c,d]
1	**Ph$_{Br}$** (49.5)	**NAP$_{Bpin}$** (50.5)	18 h	poly-**5**	93 (37)	1.48 (2.65)	3.59 (3.57)	20 (36)
2	**Ph$_{Br}$** (49.5)	**NAP$_{Bpin}$** (50.5)	5 min	poly-**5**-8.9K	95	0.89	1.42	12

[a] [**NAP$_{Bpin}$**] = 0.13 M, [P(*t*-Bu)$_3$ Pd G2] = 13 mM, [P(*t*-Bu)$_3$ Pd G2]/[K$_3$PO$_4$] = 1/58. [b] Methanol insoluble part. [c] Estimated by SEC (polystyrene standards) with chloroform as the eluent. In parentheses are shown the values estimated after SEC fractionation. [d] Number-average degree of polymerization (DP_n) estimated by M_n.

Analytical data of poly-**5**: Pale yellow solid. IR (KBr, cm^{-1}): 2200 (C≡C). ^{1}H NMR (500 MHz, 1,1,2,2-tetrachloroethane-d_2, 95 °C): δ 8.40-7.30 (br, 8H, Ar–H), 6.70-6.20 (br, 4H, Ar–H), 4.40-3.90 (br, 2H, OCH), 2.30-1.80 (br, 12H, Ar–CH$_3$), 1.80-1.55 (br, 8H, CH$_2$), 1.55-1.20 (br, 16H, CH$_2$), 1.10-0.70 (m, 12H, CH$_3$).

Analytical data of poly-**5**-8.9K: Pale yellow solid. IR (KBr, cm^{-1}): 2201 (C≡C). ^{1}H NMR (500 MHz, 1,1,2,2-tetrachloroethane-d_2, 95 °C): δ 8.30-7.40 (br, 8H, Ar–H), 6.70-6.20 (br, 4H, Ar–H), 4.40-3.90 (br, 2H, OCH), 2.20-1.80 (br, 12H, Ar–CH$_3$), 1.80-1.55 (br, 8H, CH$_2$), 1.55-1.20 (br, 16H, CH$_2$), 1.10-0.70 (m, 12H, CH$_3$).

Alkyne Benzannulation of Precursor Polymers. Alkyne benzannulations of the precursor polymers (poly-**5** and poly-**5**-8.9K) with TFA were carried out according to Fig. 3a and Supplementary Scheme 3 in a dry Schlenk flask under a dry nitrogen atmosphere in a similar way as reported previously.[S2] The resulting poly-**6** and poly-**6**-8.5K showed good solubility in common organic solvents, such as toluene, THF, and chloroform, probably due to the nonplanarity derived from the [4]helicene repeating units as well as the bulky aryl pendant groups (R^2), which suppressed excessive intermolecular interactions. The M_n and M_w/M_n values of the poly[4]helicenes were estimated by SEC using polystyrene standards in chloroform.

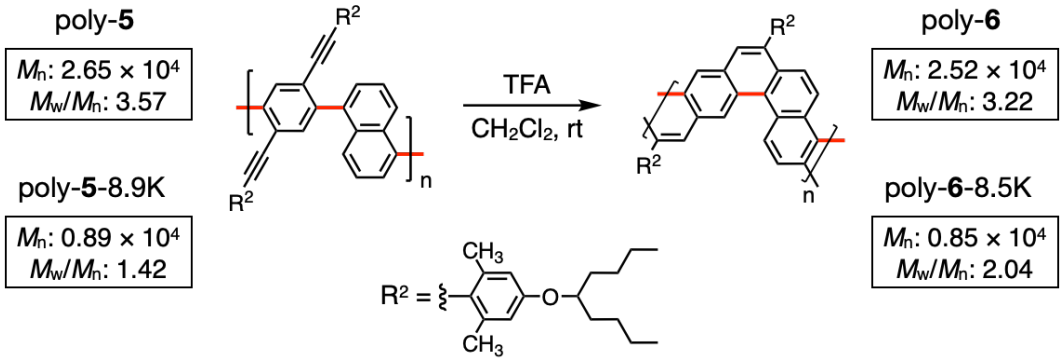

Supplementary Scheme 3 | Synthesis of poly-**6** and poly-**6**-8.5K.

Analytical data of poly-**6**: Pale yellow solid. Yield: 97%. ^{1}H NMR (500 MHz, 1,1,2,2-tetrachloroethane-d_2, 95 °C): δ 10.30-8.80 (br, 4H, Ar–H), 8.40-7.20 (br, 4H, Ar–H), 7.20-6.20 (br, 4H, Ar–H), 4.60-3.80 (br, 2H, OCH), 2.40-1.85 (br, 12H, Ar–CH_3), 1.85-1.20 (br, 24H, CH_2), 1.10-0.60 (br, 12H, CH_3).

Analytical data of poly-**6**-8.5K: Pale yellow solid. Yield: 99%. ^{1}H NMR (500 MHz, 1,1,2,2-tetrachloroethane-d_2, 95 °C): δ 10.00-8.90 (br, 4H, Ar–H), 8.20-7.40 (br, 4H, Ar–H), 7.10-6.30 (br, 4H, Ar–H), 4.50-3.80 (br, 2H, OCH), 2.40-1.90 (br, 12H, Ar–CH_3), 1.90-1.20 (br, 24H, CH_2), 1.10-0.65 (br, 12H, CH_3).

3. X-ray Crystallographic Data of Double-2

X-ray diffraction data set for double-**2** was collected on a Rigaku Saturn 724+ CCD diffractometer with Mo Kα radiation (λ = 0.71073 Å) at 93 K. Single crystals of double-**2** suitable for X-ray analysis were grown by vapor diffusion of methanol into a solution of double-**2** in chloroform, and a single yellow crystal with dimensions 0.22 × 0.15 × 0.08 mm^3 was selected for intensity measurements. The unit cell was monoclinic with the space group $P2_1/c$. Lattice constants with Z = 4, ρ_{calcd} = 1.223 g cm^{-3}, μ(Mo$_{K\alpha}$) = 0.072 mm^{-1}, F(000) = 1,560, 2θ_{max} = 60.848° were a = 16.2348(3) Å, b = 11.5347(2), c = 22.0250(4) Å, α = 90°, β = 105.712(2)°, γ = 90° and V = 3970.37(13) Å^3. A total of 32,313 reflections was collected, of which 9,576 reflections were independent (R_{int} = 0.0464). The structure was refined to final R_1 = 0.0730 for 6,828 data [I>2σ(I)] with 511 parameters and wR_2 = 0.2191 for all data, GOF = 1.045, and residual electron density max/min = 0.657/–0.251 e Å^{-3}. The ORTEP drawing is shown in Supplementary Fig. 1, and crystal data and structure refinement are listed in Supplementary Table 2.

Data collection and processing were conducted using the Rigaku CrysAlisPro software package.[S4] The structure was solved by direct methods using SHLEXT-2018/2[S5,S6] and refined by full-matrix least squares methods with SHELXL-2018/3 program[S7,S8] using Olex2-1.3.[S9] All non-hydrogen atoms were refined anisotropically. All hydrogen atoms were calculated geometrically and refined using the riding model. Crystallographic data have been deposited at the CCDC (12 Union Road, Cambridge CB2 1EZ, UK) and copies can be obtained on request, free of charge, by quoting the publication citation and the deposition number 2235844.

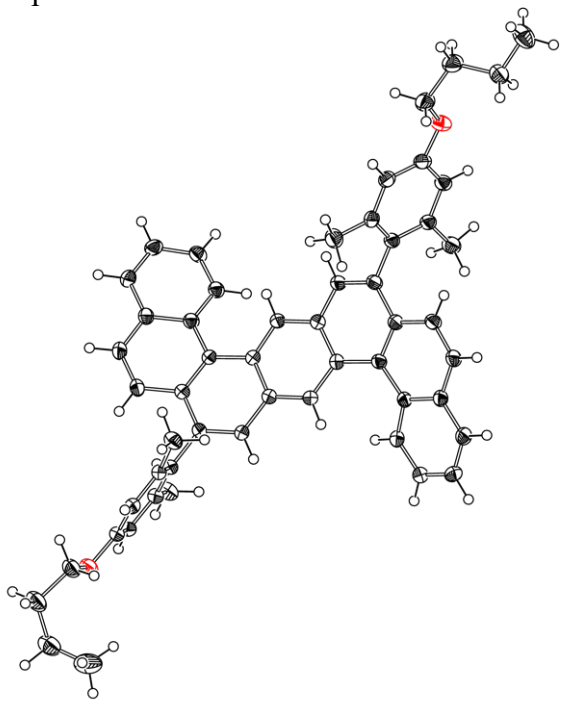

Supplementary Fig. 1 | ORTEP drawing of the crystal structure of double-**2** with thermal ellipsoids at 50% probability.

Supplementary Table 2: Crystal data and structure refinement for double-**2**.

Empirical formula	$C_{54}H_{50}O_2$	
Formula weight	730.94	
Temperature	93 K	
Wavelength	0.71073 Å	
Crystal system	monoclinic	
Space group	$P2_1/c$	
Unit cell dimensions	a = 16.2348(3) Å	α = 90°
	b = 11.5347(2) Å	β = 105.712(2)°
	c = 22.0250(4) Å	γ = 90°
Volume	3970.37(13) Å^3	
Z	4	
Density (calculated)	1.223 g cm^{-3}	
Absorption coefficient	0.072 mm^{-1}	
F(000)	1,560	
Crystal size	0.22 × 0.15 × 0.08 mm^3	
Theta range for data collection	1.905 to 30.424°	
Reflections collected	32,313	
Independent reflections	9,576 [R_{int} = 0.0464]	
Parameters	511	
Goodness-of-fit on F^2	1.045	
Final R indices [I>2sigma(I)]	R_1 = 0.0730, wR_2 = 0.1917	
R indices (all data)	R_1 = 0.1003, wR_2 = 0.2191	
Largest diff. peak and hole	0.657 and –0.251 eÅ^{-3}	
CCDC reference number	2235844	

4. Molecular Dynamics (MD) Simulations of the [4]Helicene-Based Graphene Nanoribbon (Poly-6)

4-1. Preparation for MD Simulation

MD simulations were carried out under periodic boundary conditions using GROMACS version 2020.5.[S10-12] The geometries of the repeating monomer units of poly-**6**, in which the alkoxyphenyl (R^2) groups were replaced by hydrogen atoms for simplicity, and chloroform were optimized using density functional theory (DFT) at B3LYP/6-311+G(d) level of theory.[S13-15] The Mulliken atomic charges were obtained from the single point calculation at HF/6-31G(d) level of theory using the optimized structures. The optimization and charge evaluation were conducted using Gaussian 16 program package.[S16] Using the obtained geometries and charges, the amber topology files were generated by the antechamber package[S17] with General AMBER force field (GAFF).[S18] The amber topology files were converted into a GROMACS format using the python script, Acpype.[S19]

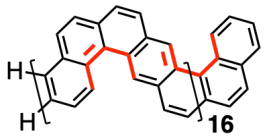

hexadeca-**6**-H containing 32 [4]helicene units
(16-mer model of poly-**6** without aryl pendants)

4-2. MD Simulations

The single polymer chain (16-mer; hexadeca-**6**-H) containing 32 alternating right (*P*)- and left (*M*)-handed helical [4]helicene units was located at the center of 30 Å cubic box including 278,421 solvent molecules of chloroform. The MD simulations were performed at 293 and 400 K as follows. First, the energy minimization of the systems was performed for the equilibration of the system based on the conjugate gradient algorithm with the threshold of the maximum force, 10.0 kJ/mol/nm. Second, the NVT equilibration for 20 ns was carried out for relaxation of the introduced solvent molecules followed by the NPT (P = 1.0 atm) equilibration for 20 ns with fixing the atomic positions of the polymer. Further 20 ns of equilibration was performed without fixing the polymer. Dynamics were propagated with a leapfrog integrator using a time step of 0.4 fs for the equilibration procedure. The MD simulations with the NPT ensemble at pressure of 1.0 atm were performed without any restraints for 60 ns at 293 and 400 K, and the snapshots were collected every 0.01 ns. The Nosé–Hoover[S20,S21] thermostat and the Parrinello–Rahman[S22,S23] isotropic barostat were used to regulate the temperature and pressure, respectively. Dynamics were propagated with a leapfrog integrator using a time step of 2 fs for the MD simulation, while preserving bond lengths using linear constraint solver algorithm.[S24] The cutoff value of 14 Å was assigned for non-bonded interactions. The long-range electrostatic interactions were corrected using the Particle Mesh Ewald (PME)[S25] method with a maximum spacing for the fast Fourier transform grid of 0.18 nm and an interpolation order of 6. To observe the changing of helicity (*P* or *M*) during the simulation time, 32 dihedrals angles were analyzed by the GROMACS utilities.

5. Theoretical Studies on the Structures of Tetra-6 with Different Combinations of Helicities and the Calculated CD Spectrum of All-(*M*)-Penta-6-H

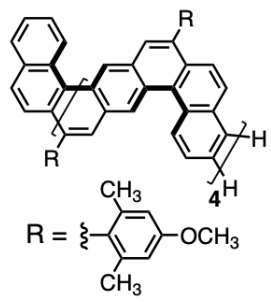

tetra-**6**

(*M*,*M*,*M*,*M*,*M*,*M*,*M*,*M*)
(*P*,*M*,*M*,*M*,*M*,*M*,*M*,*M*)
(*M*,*P*,*M*,*M*,*M*,*M*,*M*,*M*)
(*M*,*M*,*P*,*M*,*M*,*M*,*M*,*M*)
(*M*,*M*,*M*,*P*,*M*,*M*,*M*,*M*)
(*P*,*P*,*M*,*M*,*M*,*M*,*M*,*M*)
(*P*,*P*,*P*,*M*,*M*,*M*,*M*,*M*)
(*P*,*P*,*P*,*P*,*M*,*M*,*M*,*M*)
(*M*,*P*,*M*,*P*,*M*,*P*,*M*,*P*)

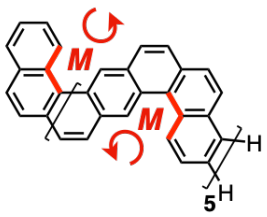

all-(*M*)-penta-**6**-H
(*M*,*M*,*M*,*M*,*M*,*M*,*M*,*M*,*M*,*M*)

The tetramer models of poly-**6** (tetra-**6**) containing methoxy groups instead of branched alkoxy groups and the pentamer model of poly-**6** (penta-**6**-H) containing hydrogen atoms instead of aryl pendants were used for the computational study for simplicity. The initial structures of tetra-**6** with different combinations of helicities and all-(*M*)-penta-**6**-H composed entirely of the (*M*)-[4]helicene-based repeating units were constructed on a Windows 10 PC with the Materials Studio Modeling software based on the bond lengths, bond angles, and internal rotation angles of the crystal structure of double-**2** (Fig. 2c,d and Supplementary Fig. 1). The structures were fully optimized by the DFT calculations using the B3LYP[S14,S15] functional with the 6-31G(d) basis sets[S26-28] in Gaussian 16 software. The theoretical CD spectrum of all (*M*)-penta-**6**-H was calculated by the time-dependent-DFT (TD-DFT) at B3LYP/6-31G(d) level of theory in Gaussian 16 software (Supplementary Fig. 23).[S29] The calculated rotational strengths in length gauge were expanded by the Gaussian functions and overlapped where the width of the band at the half-height was fixed at 0.10 eV. Computer resources for the DFT calculations were provided by the Information Technology Center of Nagoya University.

6. Molecular Modeling of Poly-6

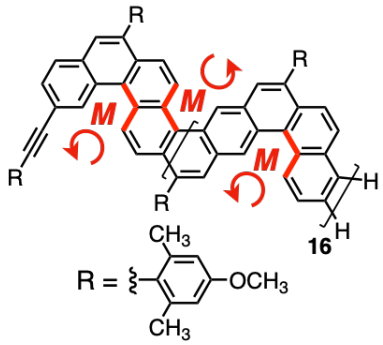

all-(*M*)-hexadeca-**6**

The molecular modeling and molecular mechanics (MM) calculations were conducted using the Compass II force field[S30] as implemented in the Materials Studio Modeling software (Version 8.0; Dassault Systèmes BIOVIA, San Diego, CA, USA) operated using a PC running under Windows 10. The polymer model of the (*M*)-handed helical poly-**6** (16 repeating monomer units) composed entirely of the (*M*)-[4]helicene-based repeating units, in which the branched alkoxy groups were replaced by the methoxy groups for simplicity, was constructed (all-(*M*)-hexadeca-**6**) by a Polymer Builder module in the Materials Studio Modeling software according to the following procedures. First, the polymer backbone was constructed based on the bond lengths, bond angles, and internal rotation angles of the crystal structure of double-**2** (Fig. 2c,d and Supplementary Fig. 1). The end group of all-(*M*)-hexadeca-**6** was then added to the polymer backbone. The dielectric constant was set to 1.0. The calculation was used with setup parameters that include a 0.001 kcal/mol/Å final convergence for minimization. The whole structure was then geometry-optimized with a cutoff distance of 18.5 Å by the conjugate gradient method.

7. Supporting Data

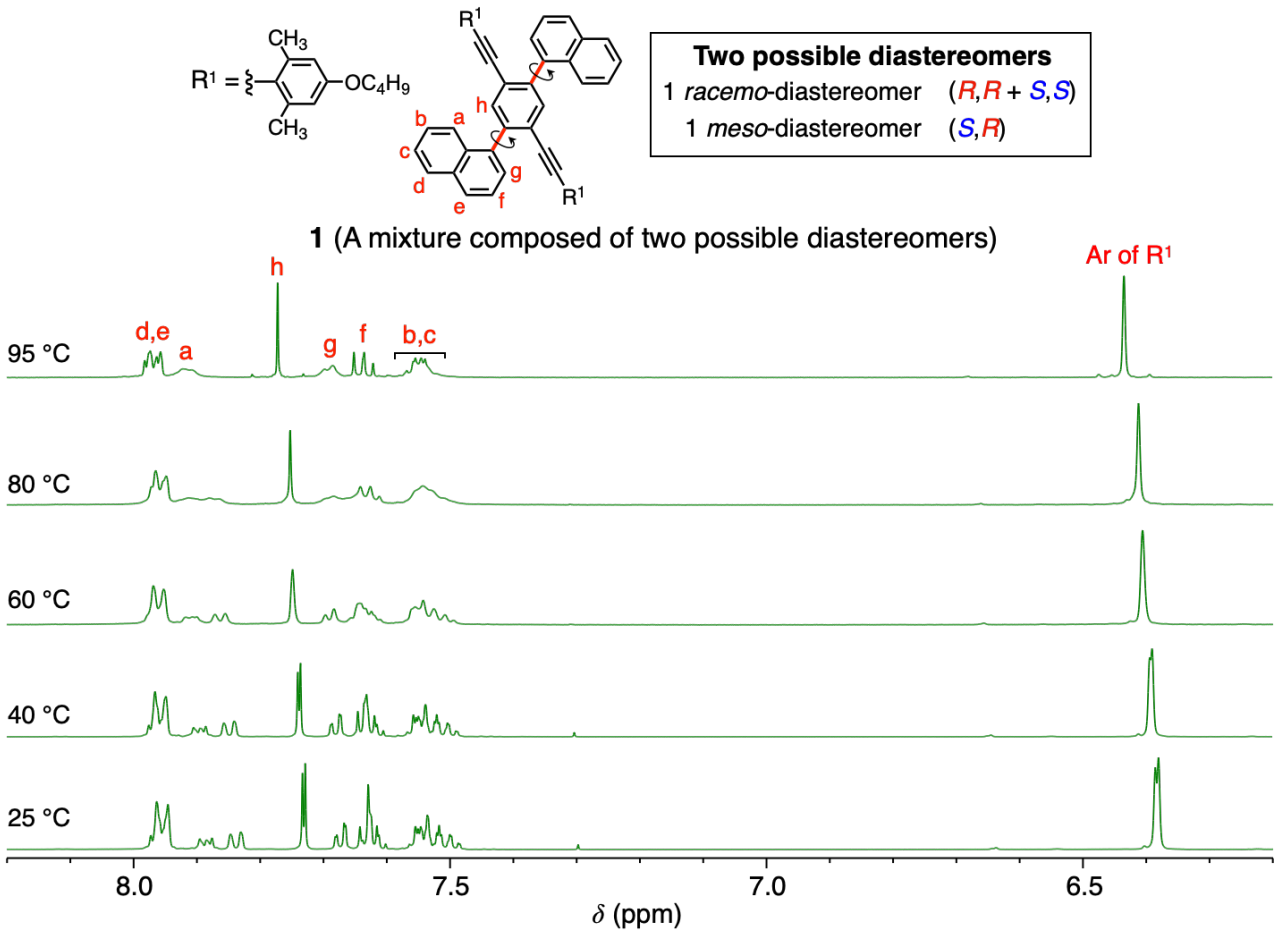

Supplementary Fig. 2 | Variable-temperature ^{1}H NMR spectra (500 MHz, 1,1,2,2-tetrachloroethane-d_2) of **1** from 25 to 95 °C. For the signal assignments, see Supplementary Fig. 4.

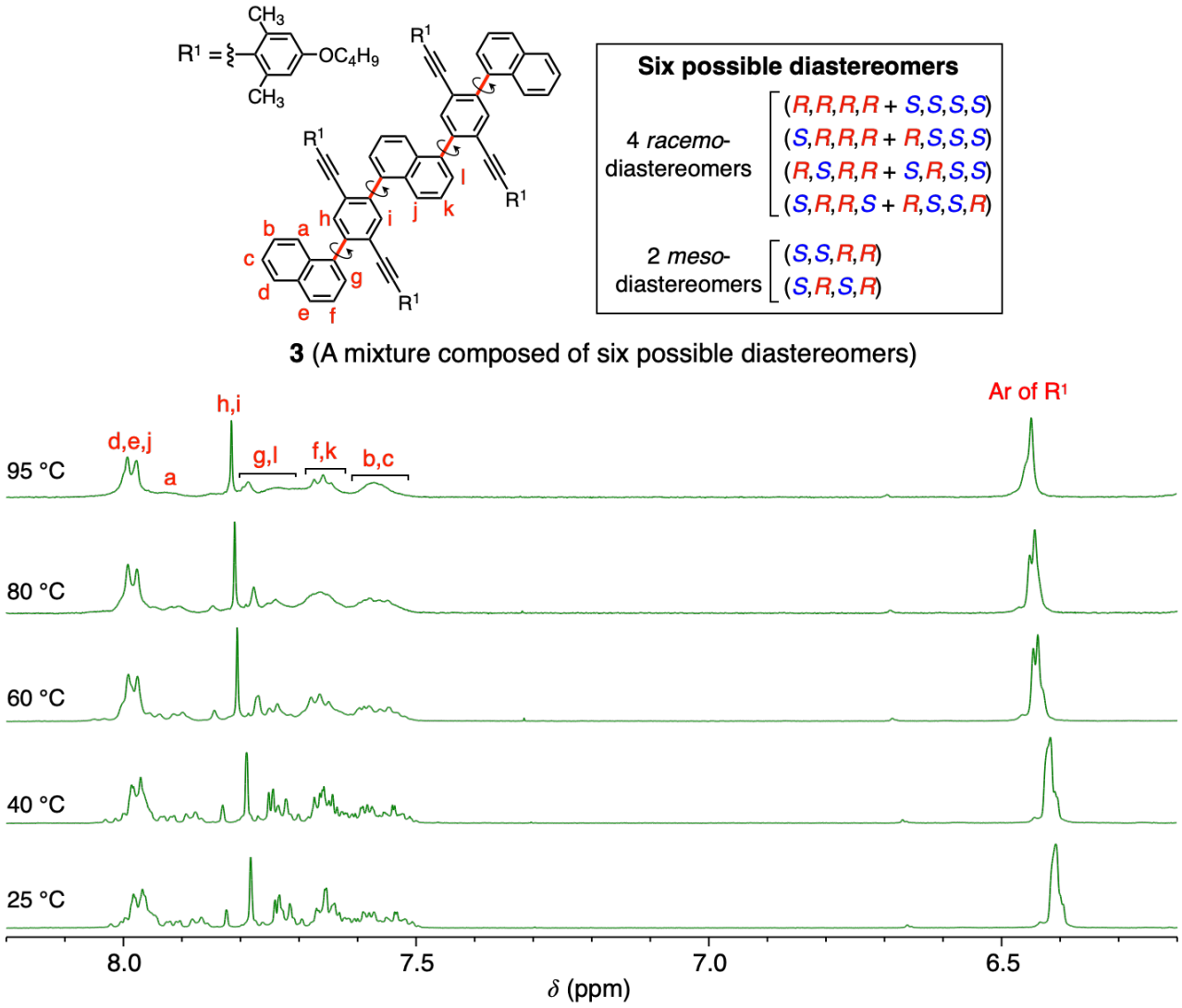

Supplementary Fig. 3 | Variable-temperature ^{1}H NMR spectra (500 MHz, 1,1,2,2-tetrachloroethane-d_2) of **3** from 25 to 95 °C. The signals were assigned based on 2D NMR experiments (Supplementary Fig. 6) and comparison with the peak assignments of **1**, **8**, and poly-**5** (Supplementary Figs. 4, 13, and 15).

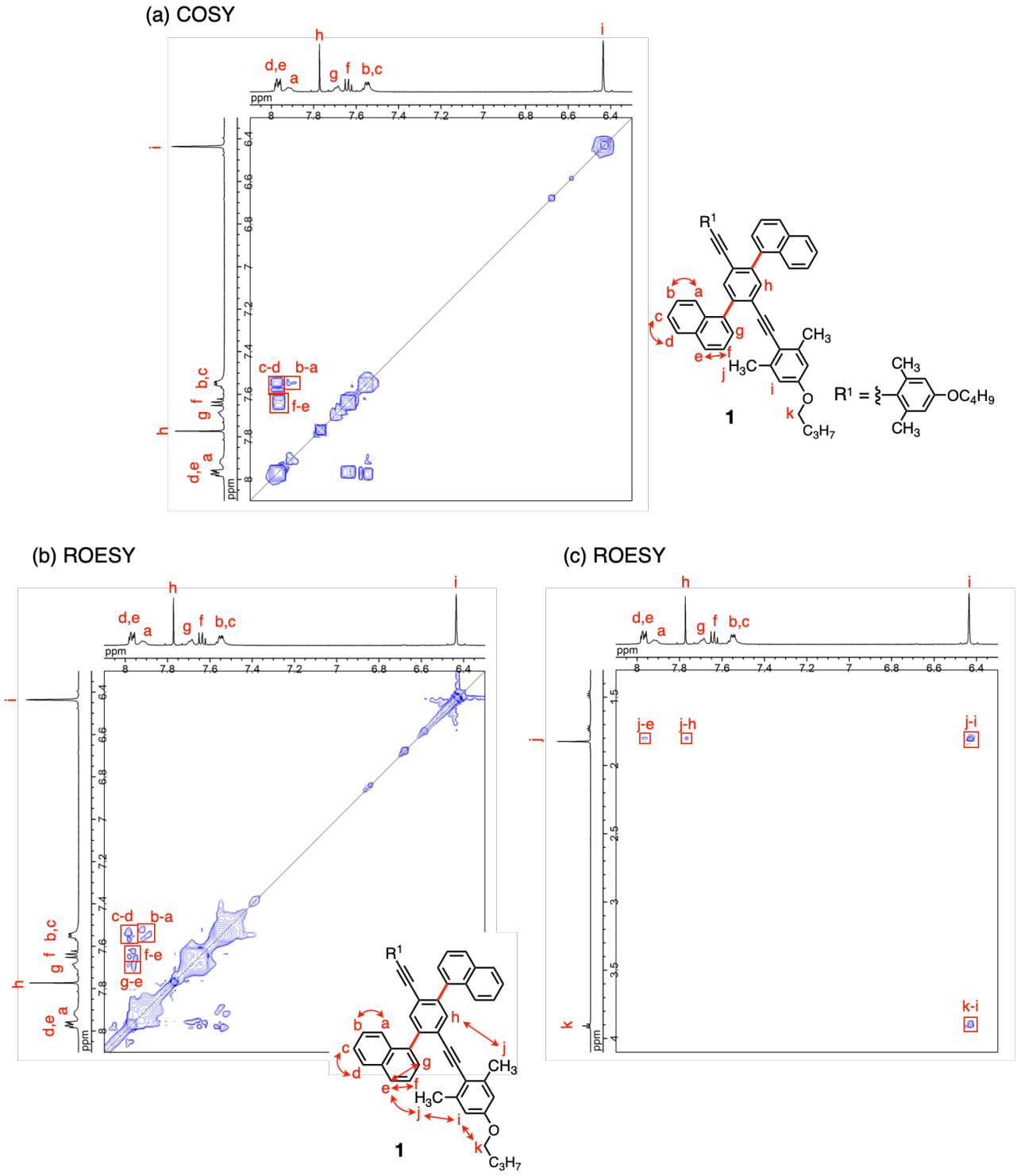

Supplementary Fig. 4 | Partial COSY (a) and ROESY (b,c) spectra (500 MHz, 1,1,2,2-tetrachloroethane-d_2, 95 °C, mixing time = 500 ms (ROESY)) of **1**.

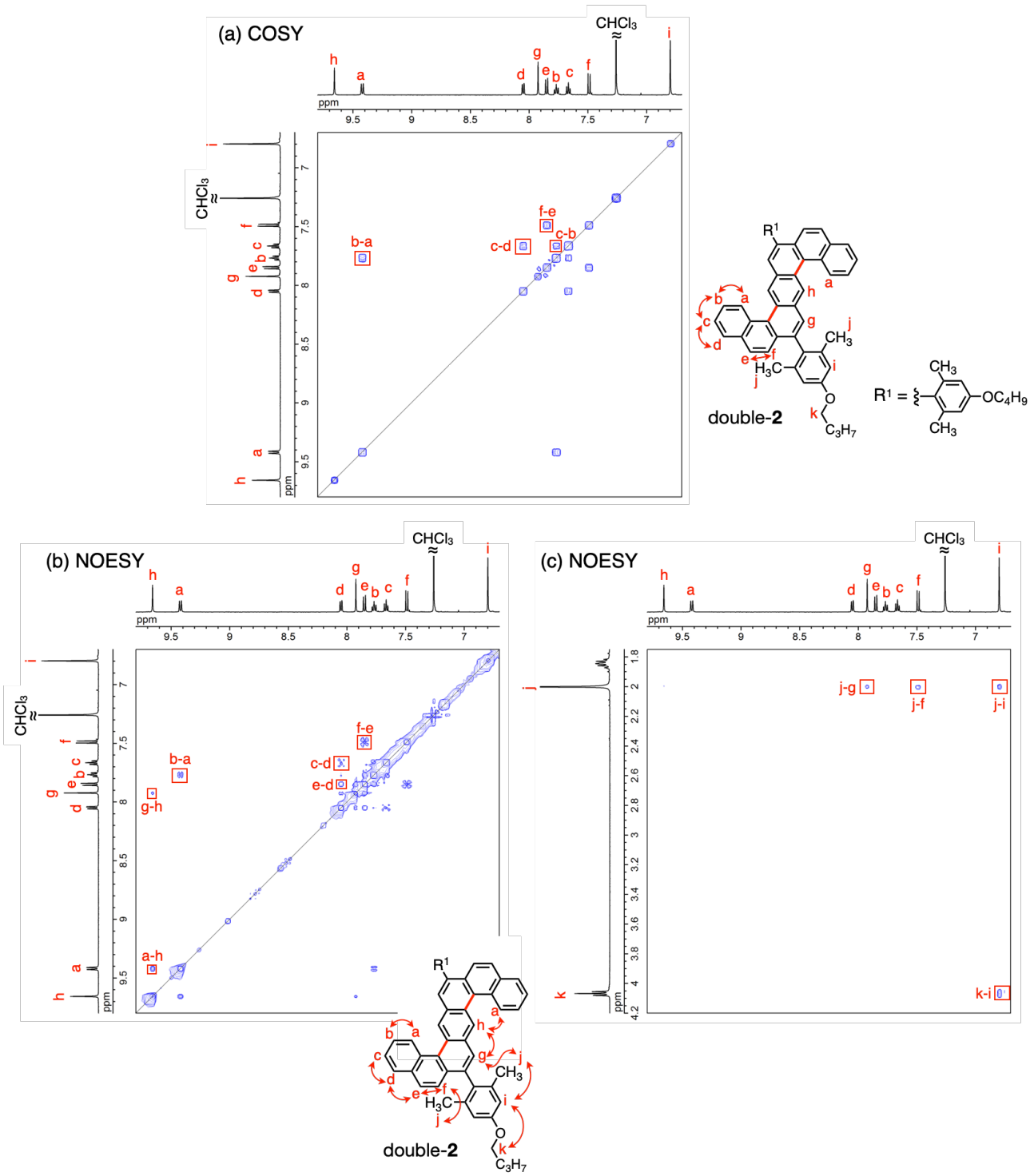

Supplementary Fig. 5 | Partial COSY (a) and NOESY (b,c) spectra (500 MHz, $CDCl_3$, room temperature, mixing time = 500 ms (NOESY)) of double-**2**.

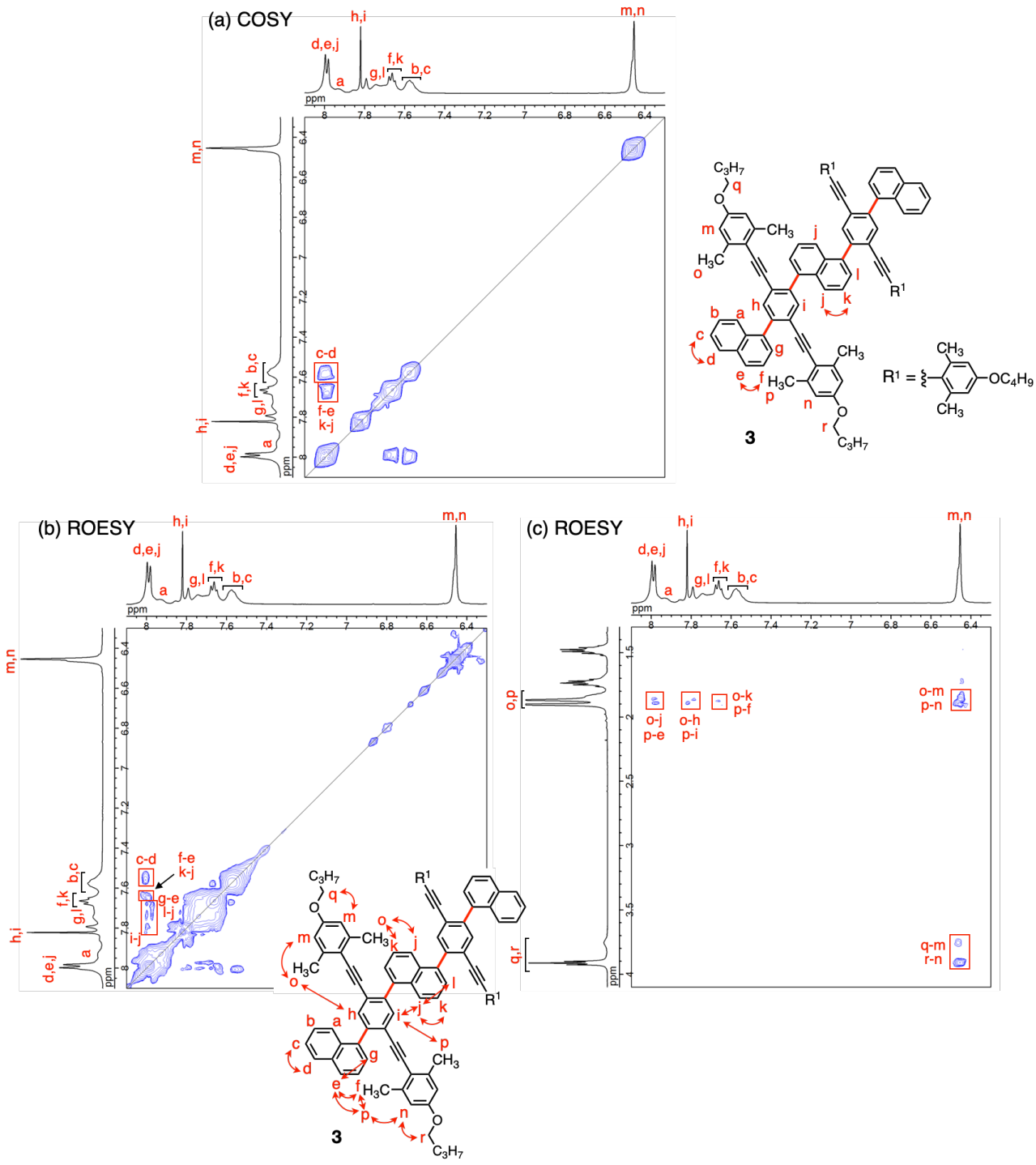

Supplementary Fig. 6 | Partial COSY (a) and ROESY (b,c) spectra (500 MHz, 1,1,2,2-tetrachloroethane-d_2, 95 °C, mixing time = 500 ms (ROESY)) of **3**.

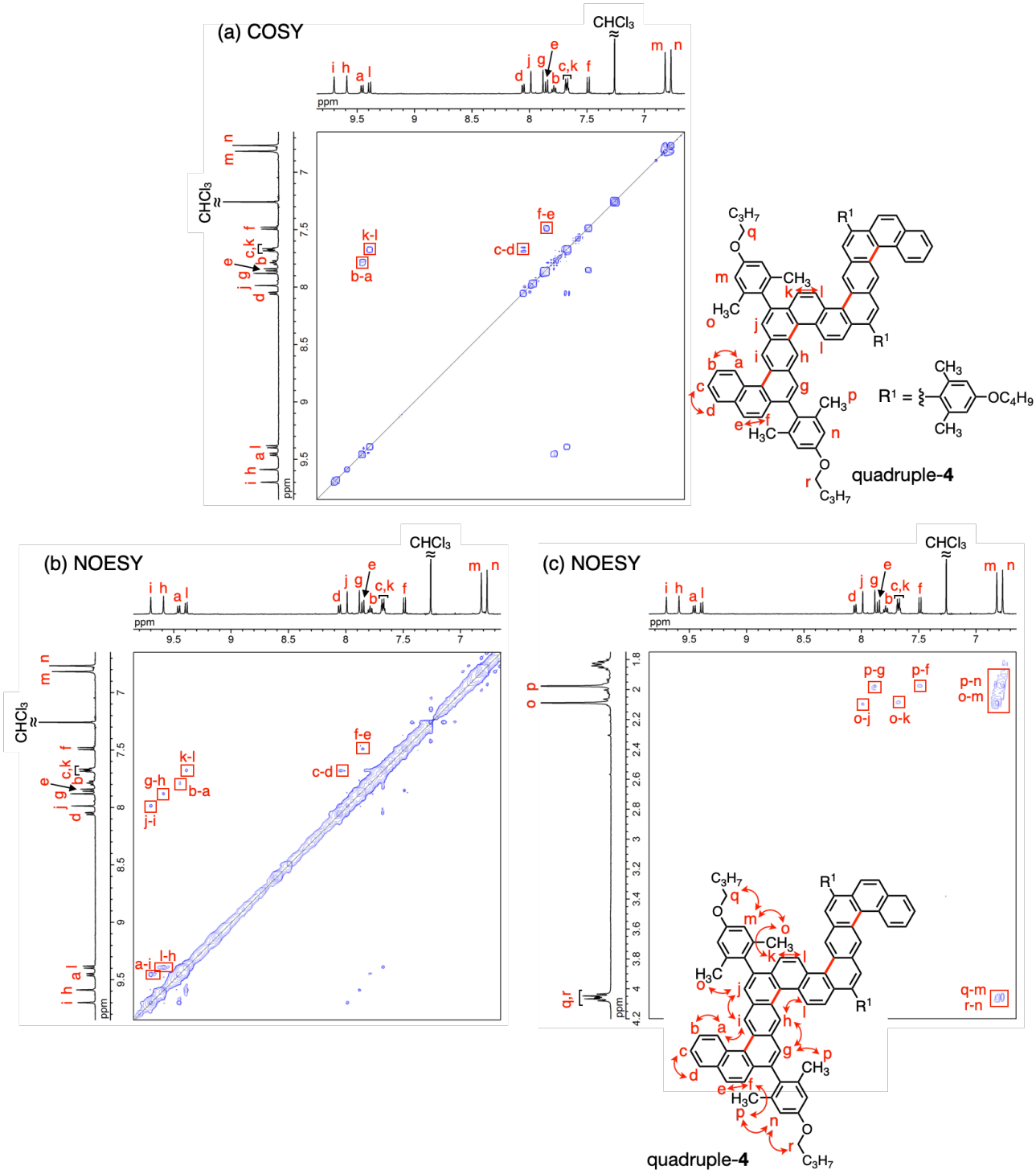

Supplementary Fig. 7 | Partial COSY (a) and NOESY (b,c) spectra (500 MHz, $CDCl_3$, room temperature, mixing time = 500 ms (NOESY)) of quadruple-**4**.

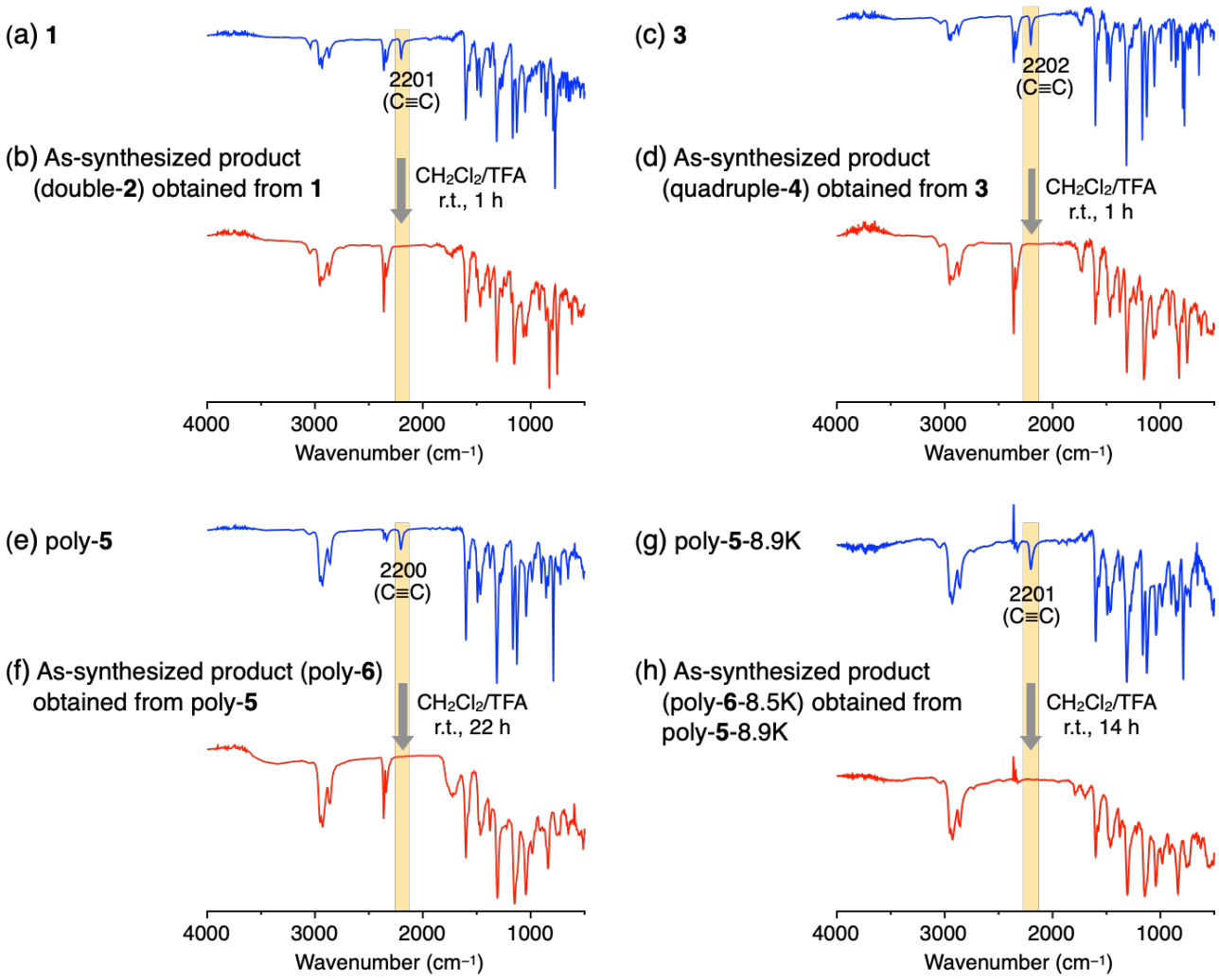

Supplementary Fig. 8 | IR spectra of **1** (a), **3** (c), poly-**5** (e), poly-**5**-8.9K (g), and those of the as-synthesized products after acid-promoted cyclizations in a dichloromethane/TFA (60/1, v/v) mixture at room temperature, measured in ATR mode at room temperature.

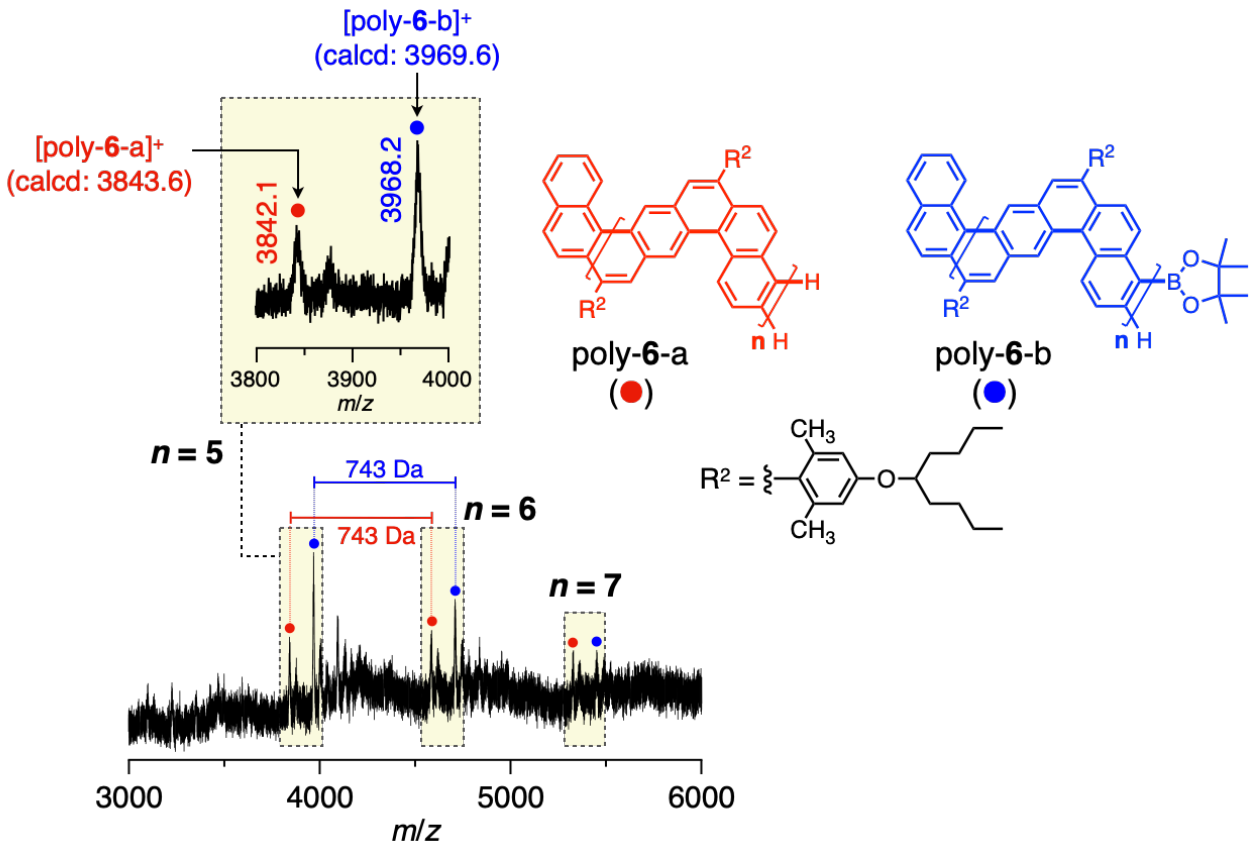

Supplementary Fig. 9 | MALDI-TOF-MS spectrum of poly-**6**. The MS measurement was performed using *trans*-2-[3-(4-*tert*-butylphenyl)-2-methyl-2-propenylidene]malononitrile as a matrix.

Because of the limited ionization efficiency of poly-**6**, its high-molar-mass components could not be detected by the MALDI-TOF-MS spectrometry, but main series of peaks with a regular interval of approximately 743 (*m*/*z*) mass, corresponding to the molar mass of the repeating [4]helicene unit, were observed in the oligomer region (DP ≤ 7).

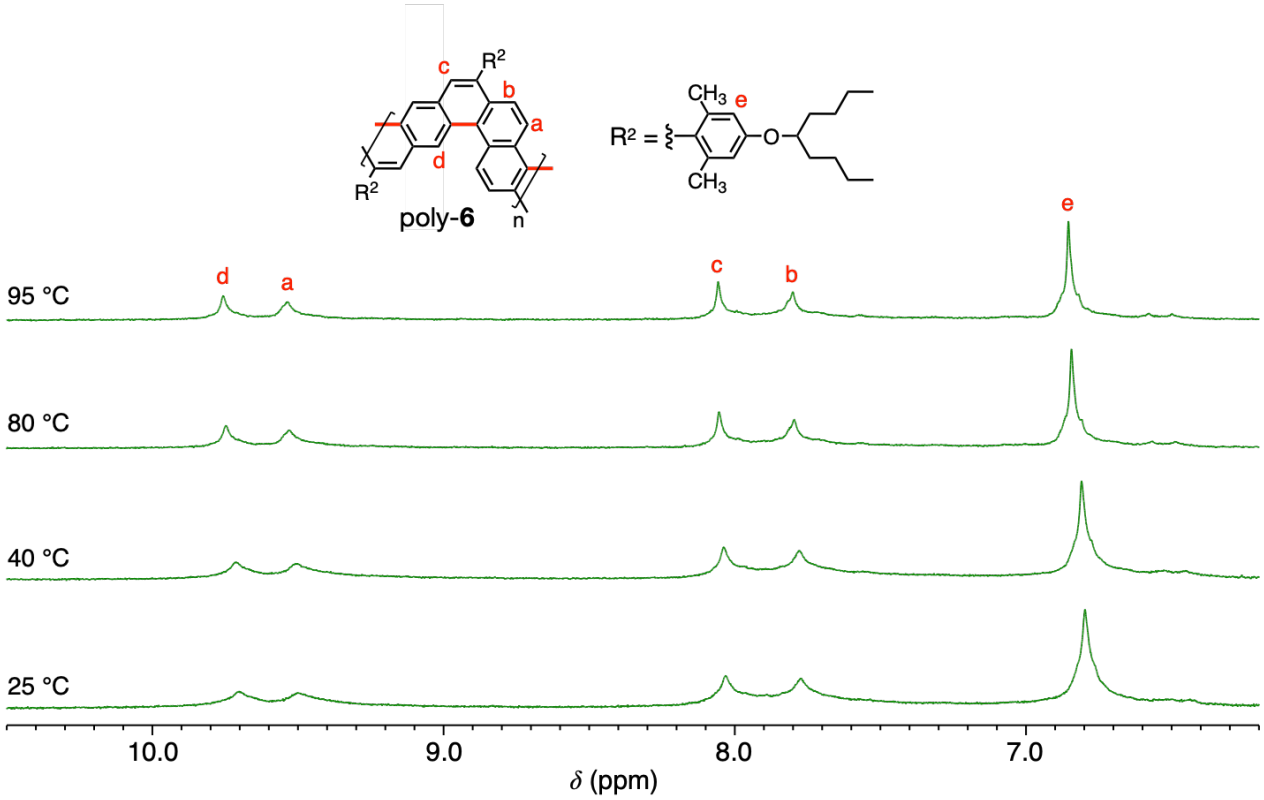

Supplementary Fig. 10 | Variable-temperature ^{1}H NMR spectra (500 MHz, 1,1,2,2-tetrachloroethane-d_2) of poly-**6** from 25 to 95 °C. For the signal assignments, see Supplementary Fig. 11.

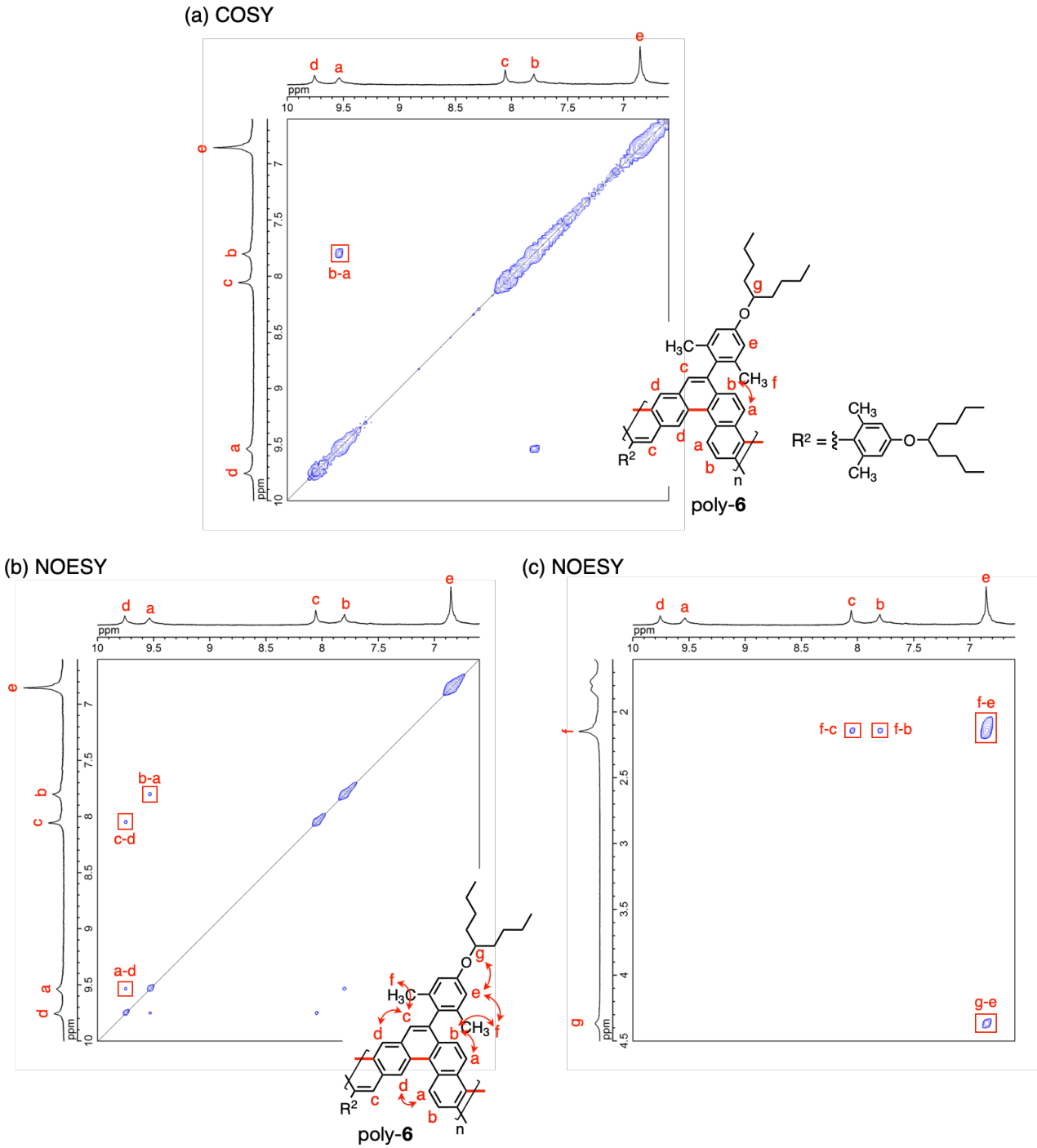

Supplementary Fig. 11 | Partial COSY (a) and NOESY (b,c) spectra (500 MHz, 1,1,2,2-tetrachloroethane-d_2, 95 °C, mixing time = 500 ms (NOESY)) of poly-**6**.

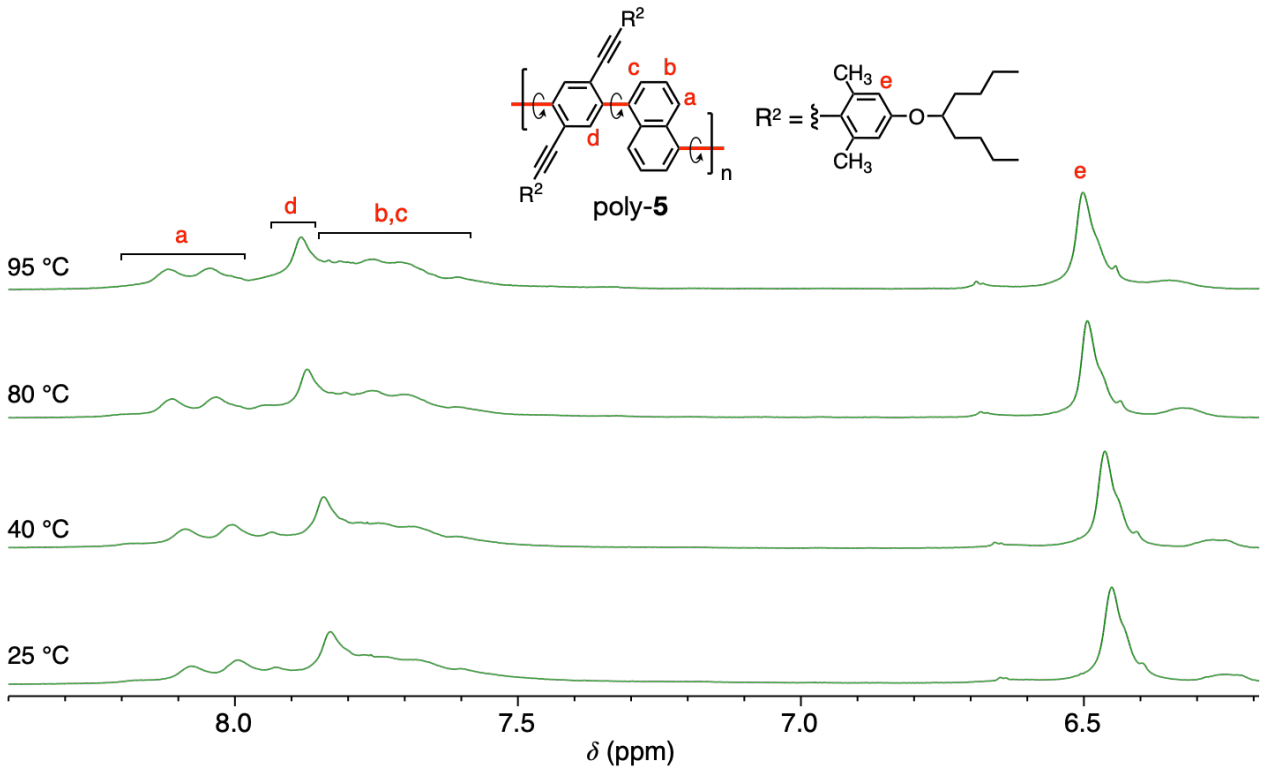

Supplementary Fig. 12 | Variable-temperature ^{1}H NMR spectra (500 MHz, 1,1,2,2-tetrachloroethane-d_2) of poly-**5** from 25 to 95 °C. For the signal assignments, see Supplementary Fig. 13.

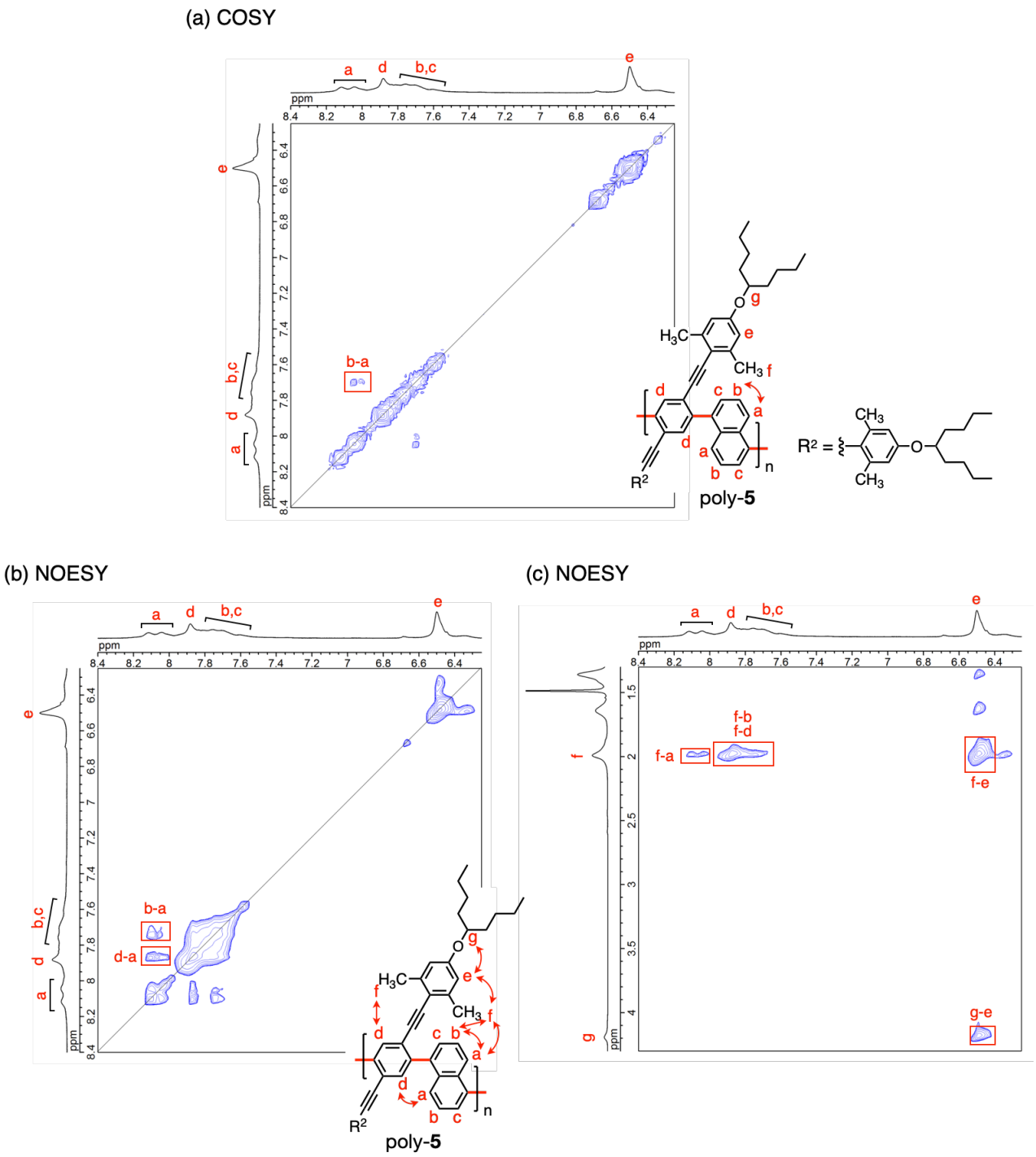

Supplementary Fig. 13 | Partial COSY (a) and NOESY (b,c) spectra (500 MHz, 1,1,2,2-tetrachloroethane-d_2, 95 °C, mixing time = 500 ms (NOESY)) of poly-**5**.

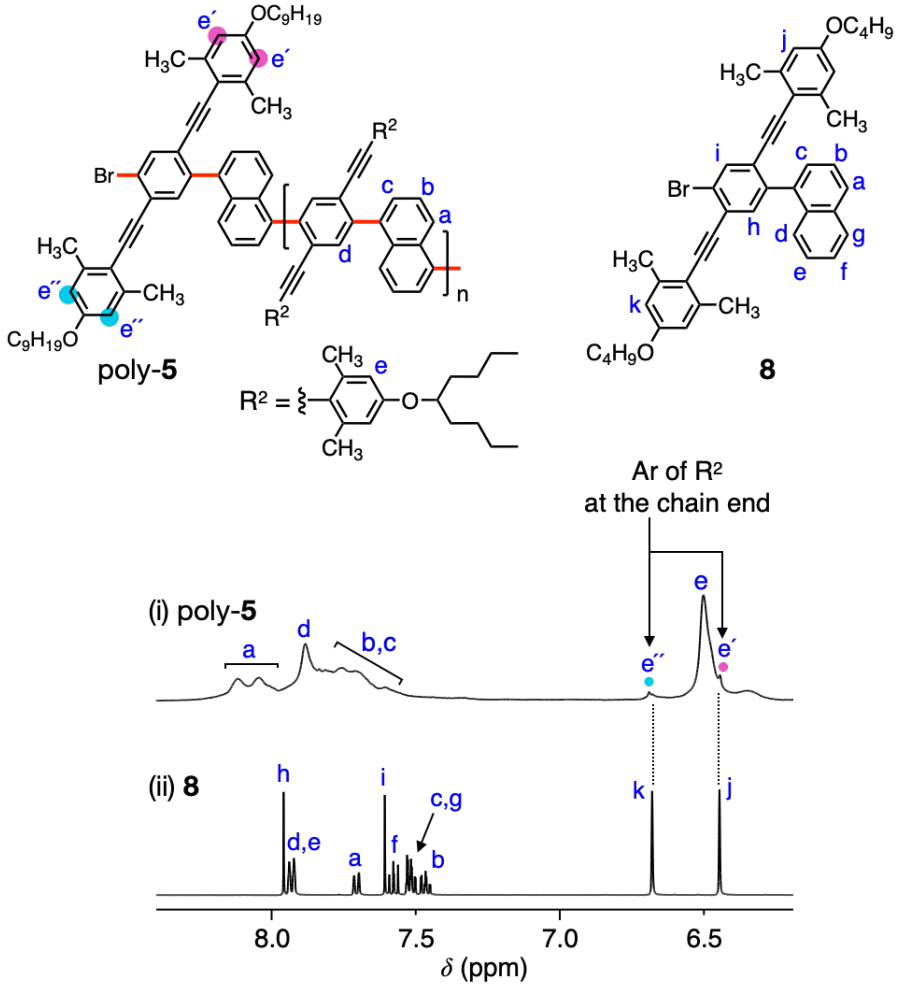

Supplementary Fig. 14 | ^{1}H NMR (500 MHz, 1,1,2,2-tetrachloroethane-d_2, 95 °C) spectra of poly-**5** (i) and **8** (ii). For the signal assignments, see Supplementary Figs. 13 and 15.

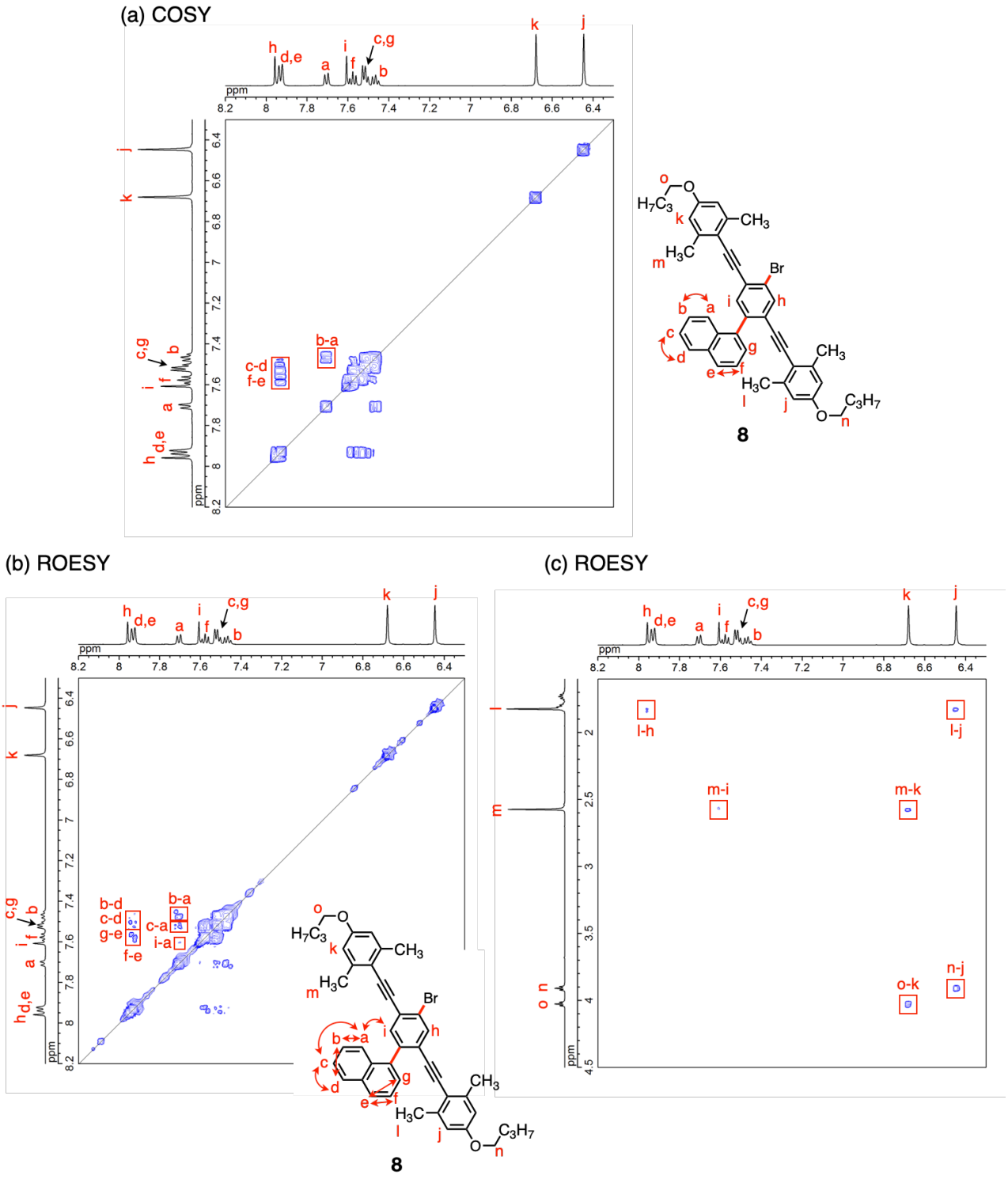

Supplementary Fig. 15 | Partial COSY (a) and ROESY (b,c) spectra (500 MHz, 1,1,2,2-tetrachloroethane-d_2, 95 °C, mixing time = 500 ms (ROESY)) of **8**.

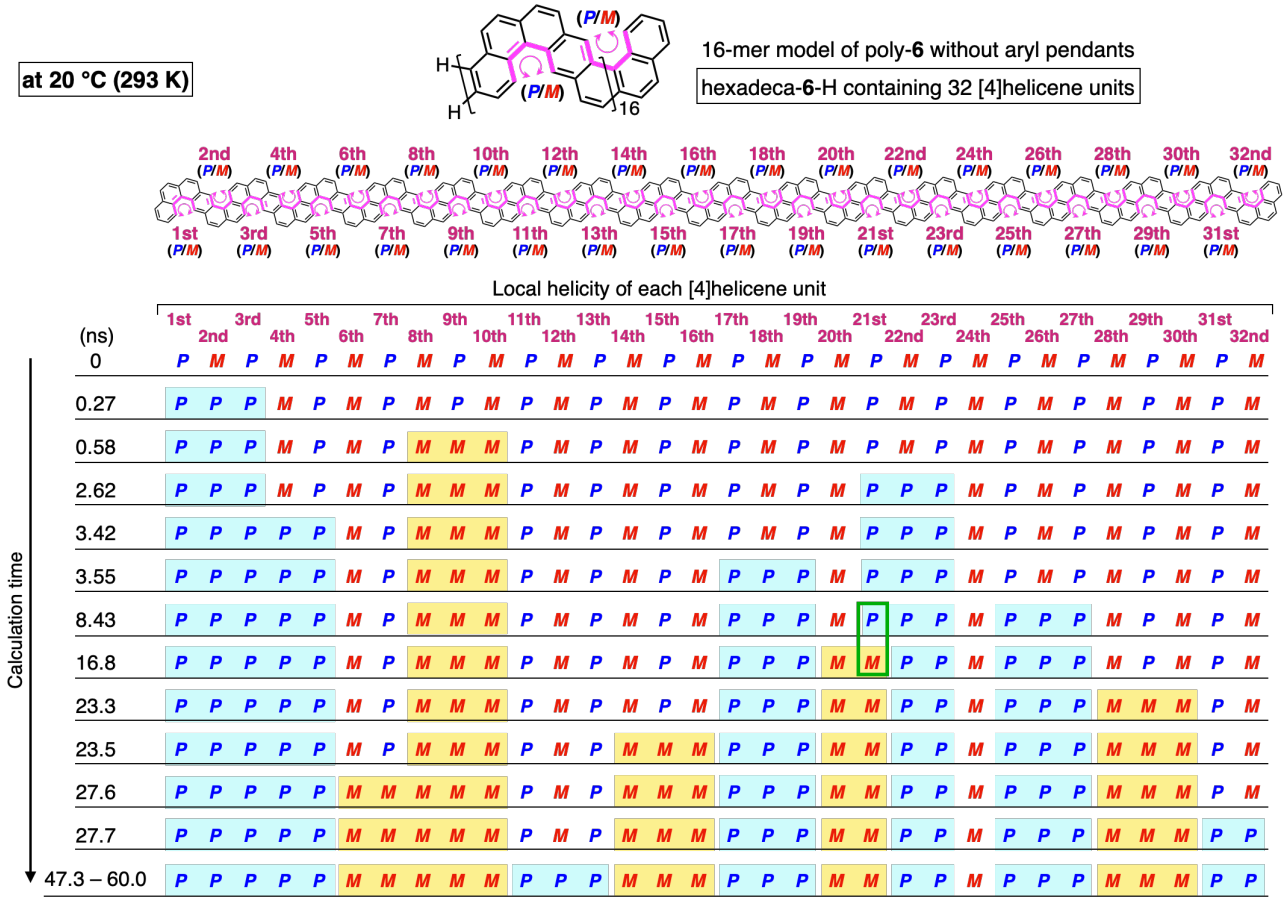

Supplementary Fig. 16 | Local helicity change of each [4]helicene unit in hexadeca-**6**-H (16-mer model of poly-**6** without aryl pendants) containing 32 [4]helicene units (1st to 32nd) during the MD simulation at 20 °C (293 K) for 60 ns. Hexadeca-**6**-H with an alternating arrangement of the (*P*)- and (*M*)-handed helical [4]helicene units was used as an initial structure. The helix-inversion occurring within the homochiral domain end is indicated by the green square. For model structures of hexadeca-**6**-H before and after the MD simulation at 20 °C (293 K) for 60 ns and details of the dihedral angle changes of each [4]helicene unit in hexadeca-**6**-H during the MD simulation, see Fig. 4a and Supplementary Fig. 17, respectively.

at 20 °C (293 K)

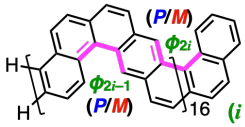

16-mer model of poly-**6** without aryl pendants

hexadeca-**6**-H containing 32 [4]helicene units

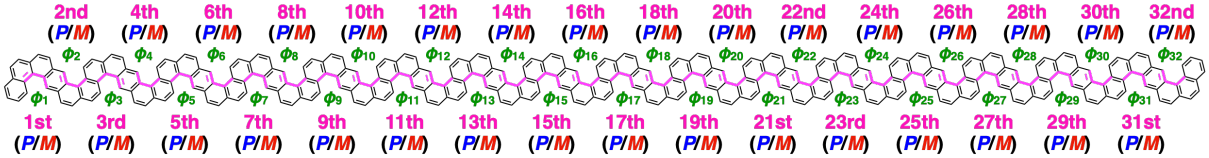

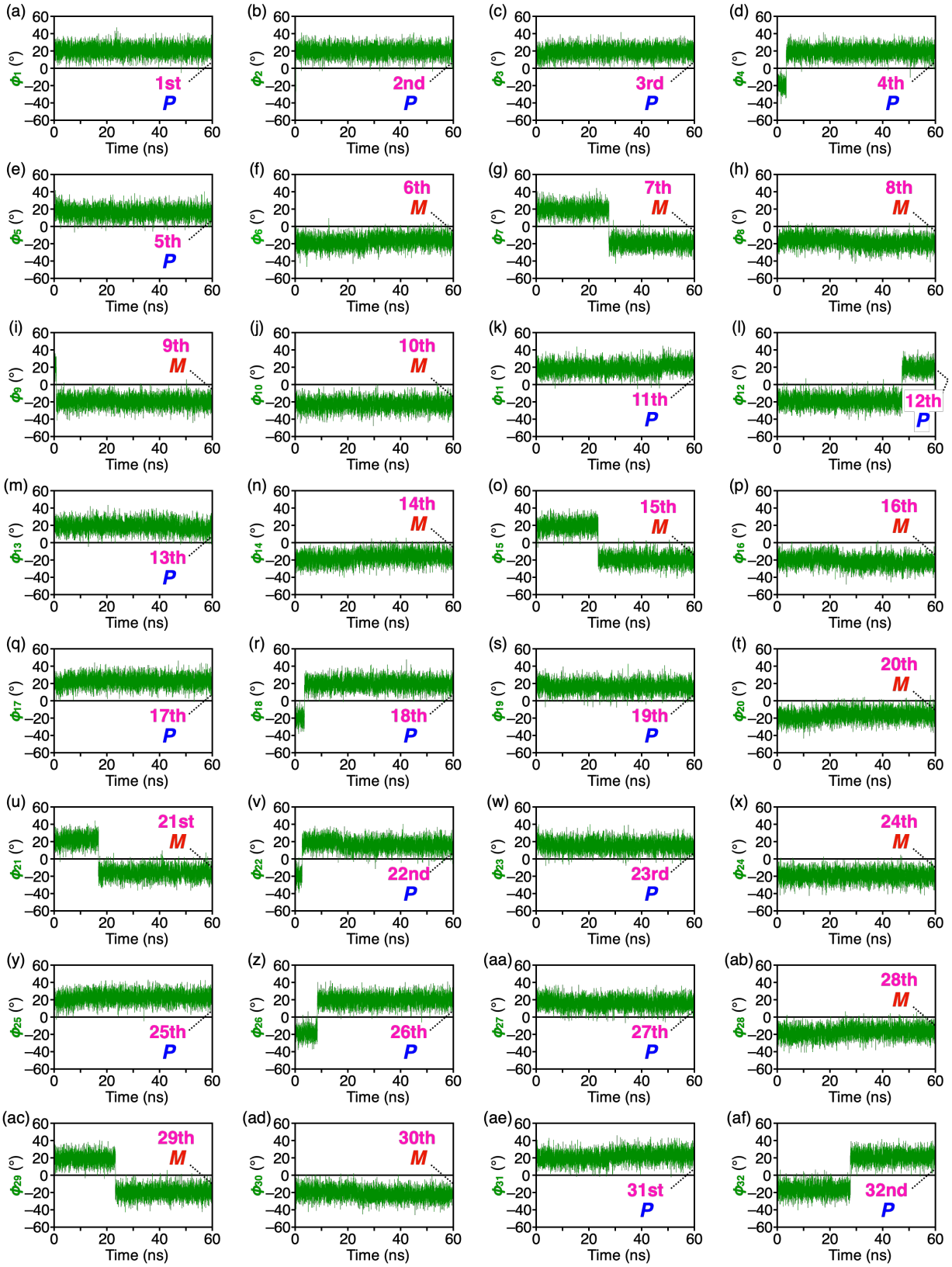

Supplementary Fig. 17 | Plots of the dihedral angles, ϕ_{2i-1} and ϕ_{2i} (i = 1 – 16), of each [4]helicene unit in hexadeca-**6**-H containing 32 [4]helicene units (1st to 32nd) during the MD simulation at 20 °C (293 K) for 60 ns. Hexadeca-**6**-H with an alternating arrangement of the (*P*)- and (*M*)-handed helical [4]helicene units was used as an initial structure.

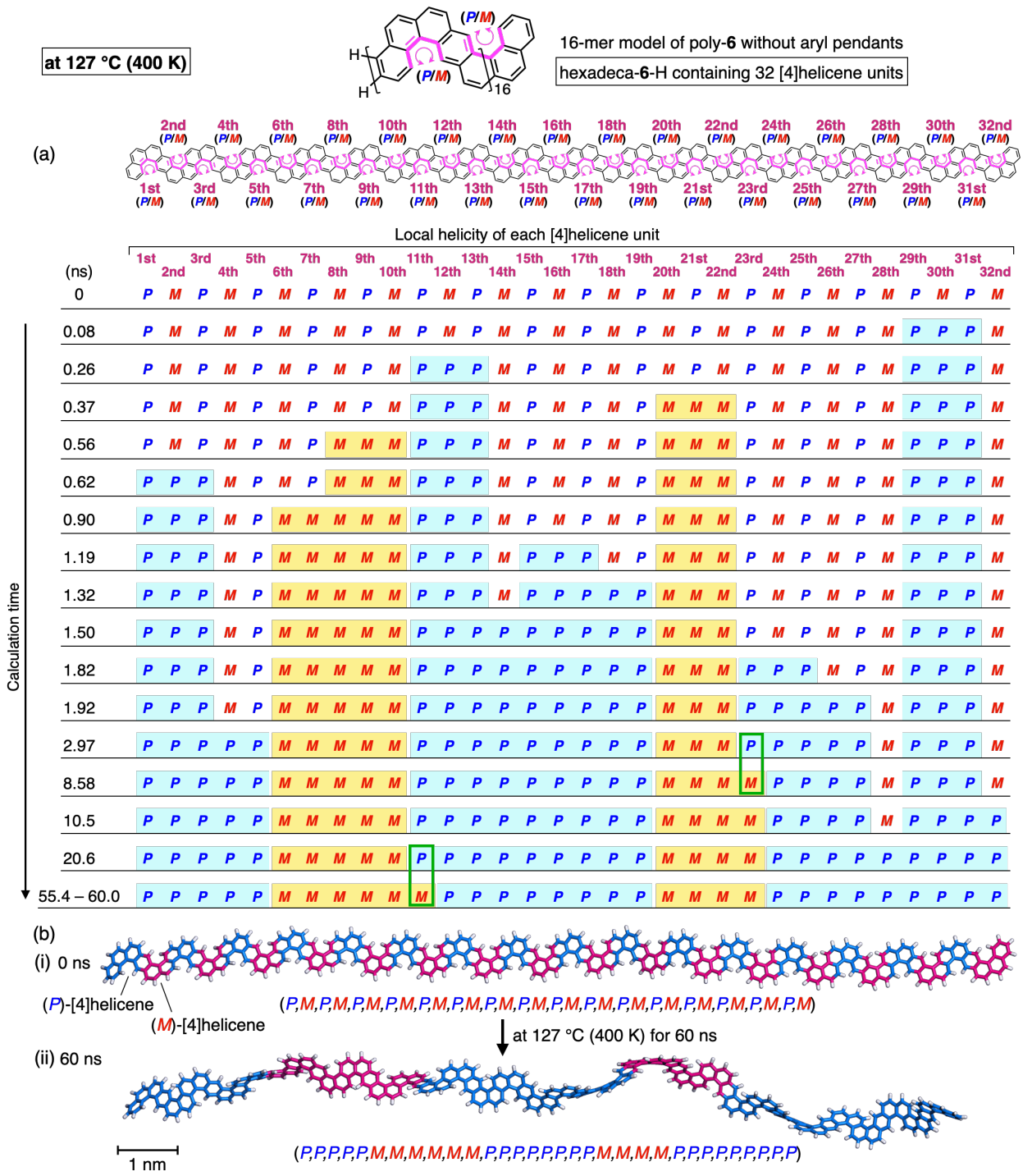

Supplementary Fig. 18 | (a) Local helicity change of each [4]helicene unit in hexadeca-**6**-H (16-mer model of poly-**6** without aryl pendants) containing 32 [4]helicene units (1st to 32nd) during the MD simulation at 127 °C (400 K) for 60 ns. Hexadeca-**6**-H with an alternating arrangement of the (*P*)- and (*M*)-handed helical [4]helicene units was used as an initial structure. The helix-inversions occurring within the homochiral domain ends are indicated by the green squares. For details of the dihedral angle changes of each [4]helicene unit in hexadeca-**6**-H during the MD simulation, see Supplementary Fig. 19. (b) Side views of hexadeca-**6**-H before (i) and after (ii) the MD simulation at 127 °C (400 K) for 60 ns. The structures are represented by capped-stick models, and the carbon atoms of the (*P*)- and (*M*)-[4]helicene units in the backbone are highlighted in blue and red, respectively, for clarity.

at 127 °C (400 K)

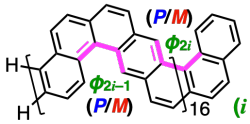

16-mer model of poly-**6** without aryl pendants

hexadeca-**6**-H containing 32 [4]helicene units

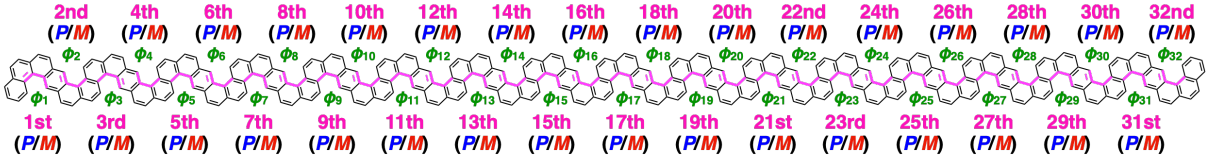

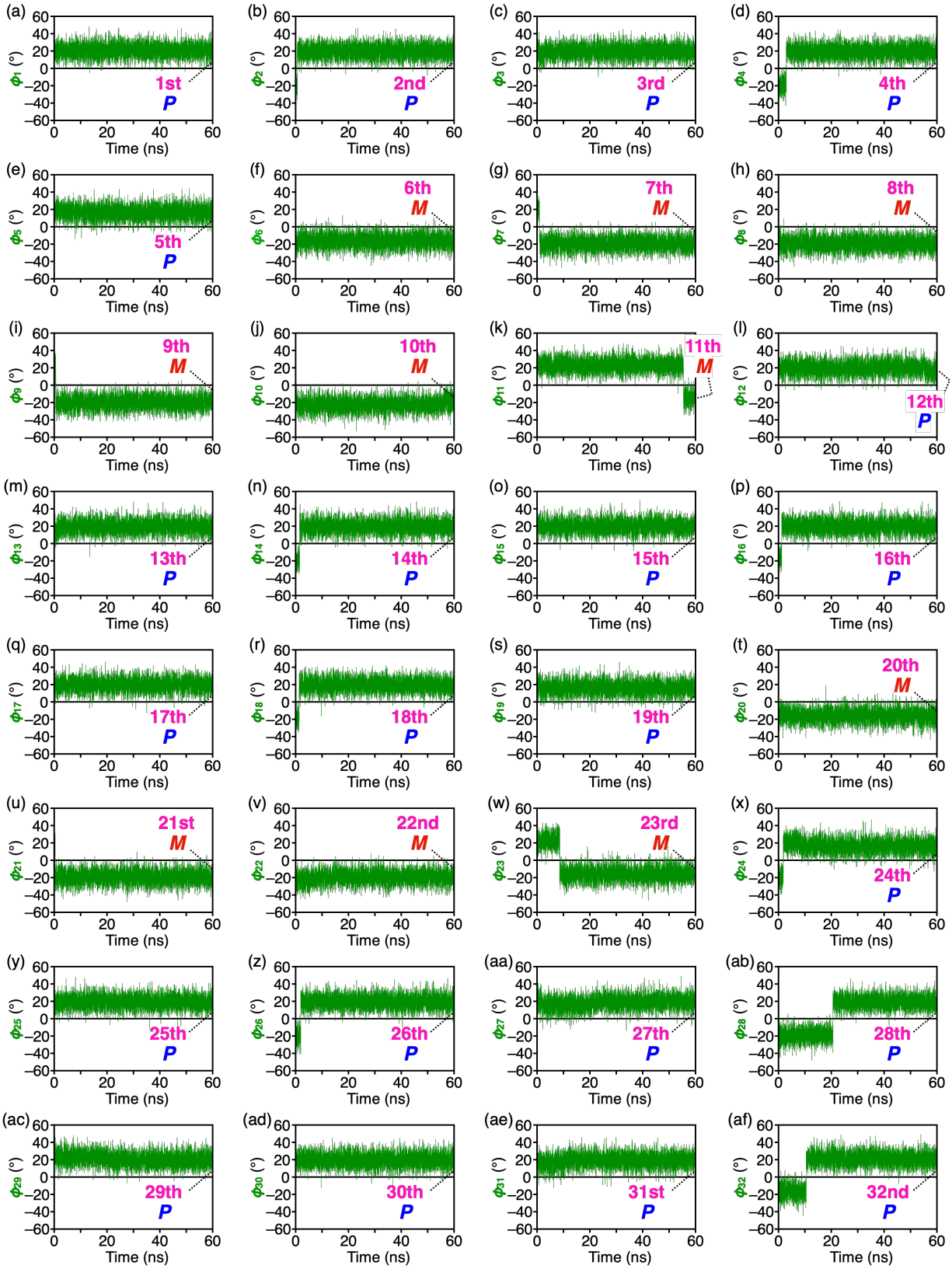

Supplementary Fig. 19 | Plots of the dihedral angles, ϕ_{2i-1} and ϕ_{2i} (i = 1 – 16), of each [4]helicene unit in hexadeca-**6**-H containing 32 [4]helicene units (1st to 32nd) during the MD simulation at 127 °C (400 K) for 60 ns. Hexadeca-**6**-H with an alternating arrangement of the (*P*)- and (*M*)-handed helical [4]helicene units was used as an initial structure.

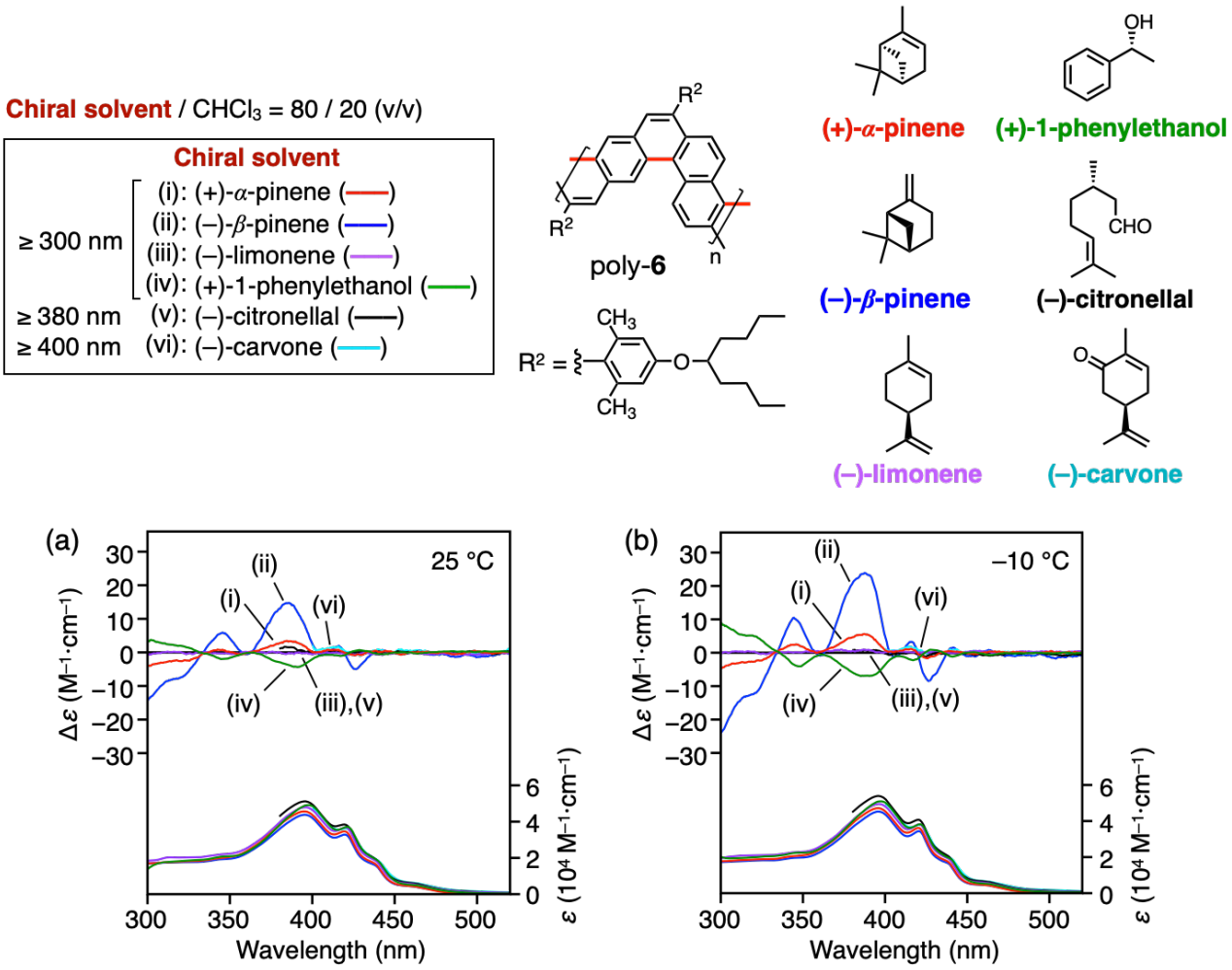

Supplementary Fig. 20 | CD and absorption spectra of poly-**6** in different chiral solvents containing chloroform (80/20, v/v) (chiral solvent: (+)-*α*-pinene (i), (–)-*β*-pinene (ii), (–)-limonene (iii), (+)-1-phenylethanol (iv), (–)-citronellal (v), and (–)-carvone (vi)) at 25 °C (a) and –10 °C (b). [Polymer] = 0.15 mM.

Because poly-**6** was not soluble in the pure chiral solvents investigated, chloroform was used as a good cosolvent to dissolve the polymer.

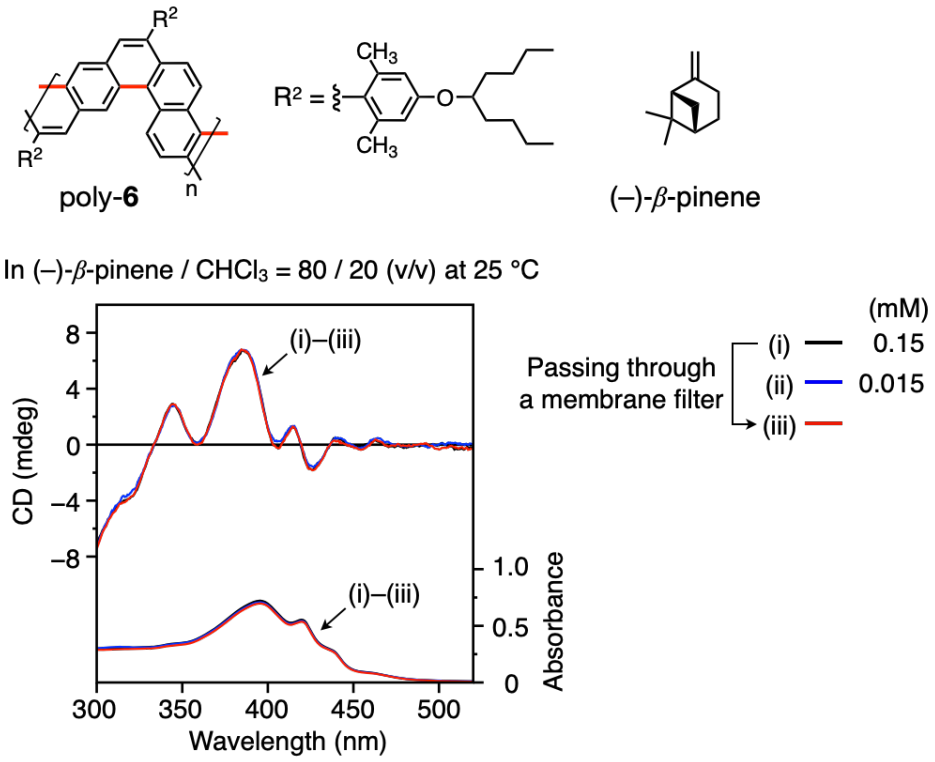

Supplementary Fig. 21 | CD and absorption spectra of poly-**6** in (–)-*β*-pinene/chloroform (80/20, v/v) at 25 °C before (i and ii) and after filtration of (i) through a membrane filter with a pore size of 0.22 *μ*m (iii). The spectra were measured in 1.0- (0.15 mM (i and iii)) and 10-mm (0.015 mM (ii)) cells.

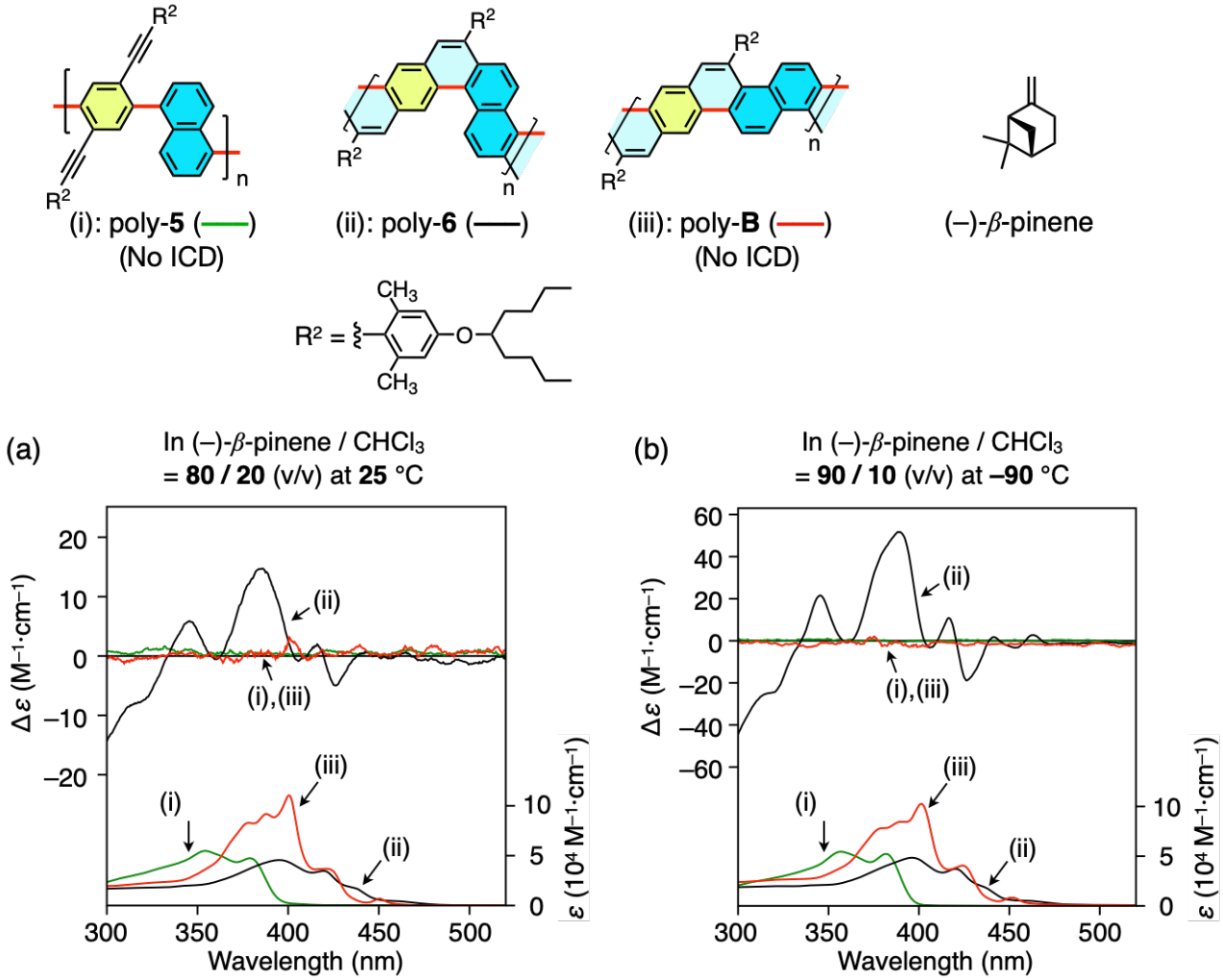

Supplementary Fig. 22 | CD and absorption spectra of poly-**5** (i), poly-**6** (ii), and poly-**B** (iii) in (–)-*β*-pinene/chloroform (80/20, v/v) at 25 °C (a) and in (–)-*β*-pinene/chloroform (90/10, v/v) at –90 °C (b). [Polymer] = 0.15 mM.

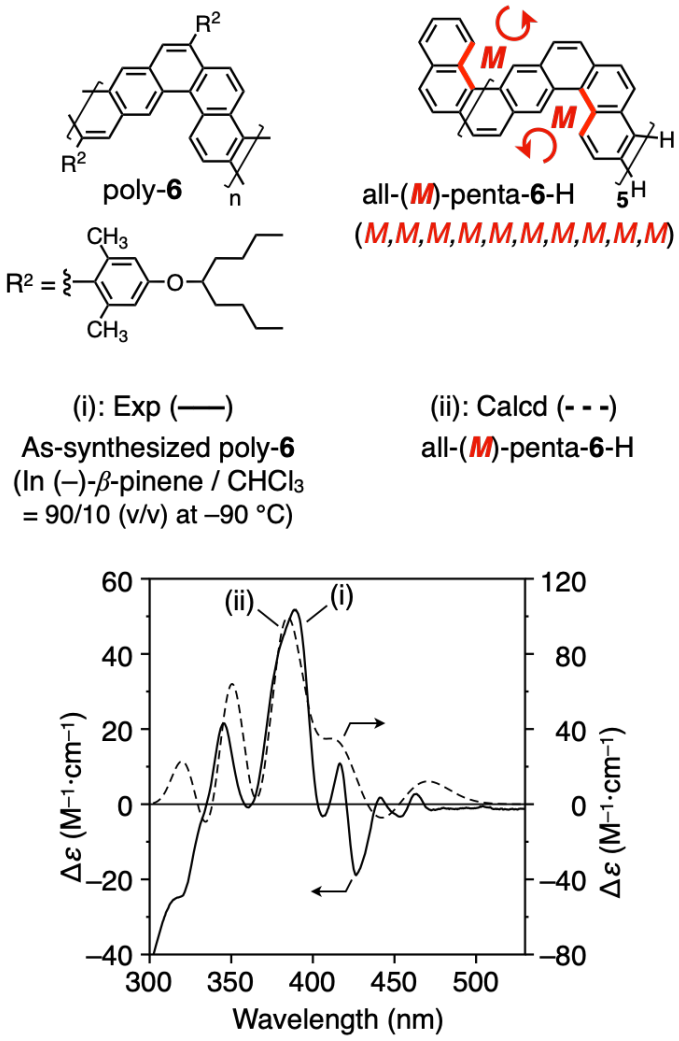

Supplementary Fig. 23 | Observed (solid lines) and calculated (dotted lines) CD spectra of poly-**6** and all-(***M***)-penta-**6**-H, respectively. The concentration of poly-**6** was calculated based on the repeating units. The calculated CD spectrum of all-(***M***)-penta-**6**-H was obtained by TD-DFT at the B3LYP/6-31G(d) level of theory and its intensity was scaled to one-fifth to express it per repeating unit.

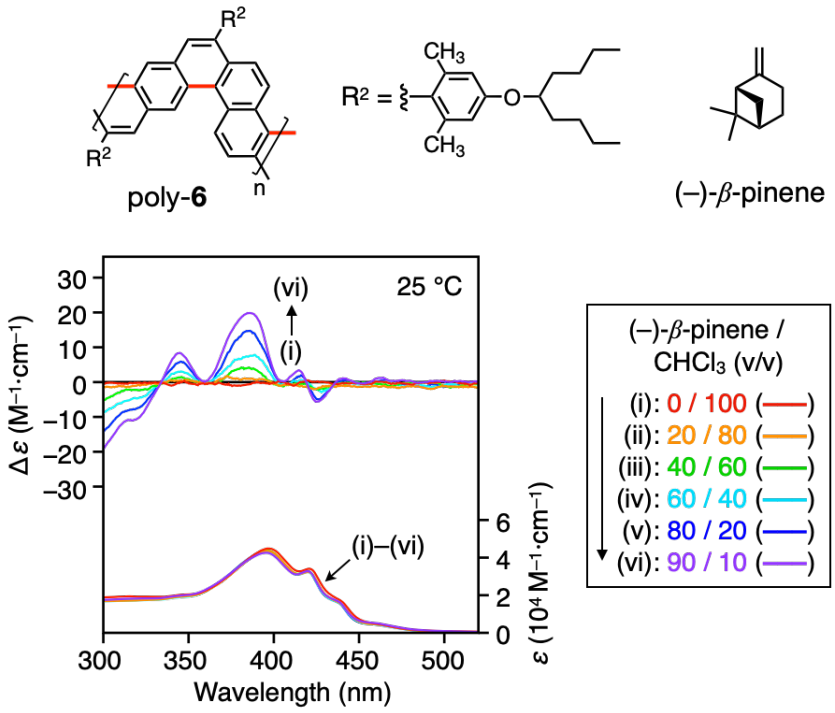

Supplementary Fig. 24 | (a) CD and absorption spectra of poly-**6** in (–)-*β*-pinene/chloroform (0/100 (i) – 90/10 (vi), v/v) at 25 °C. [Polymer] = 0.15 mM.

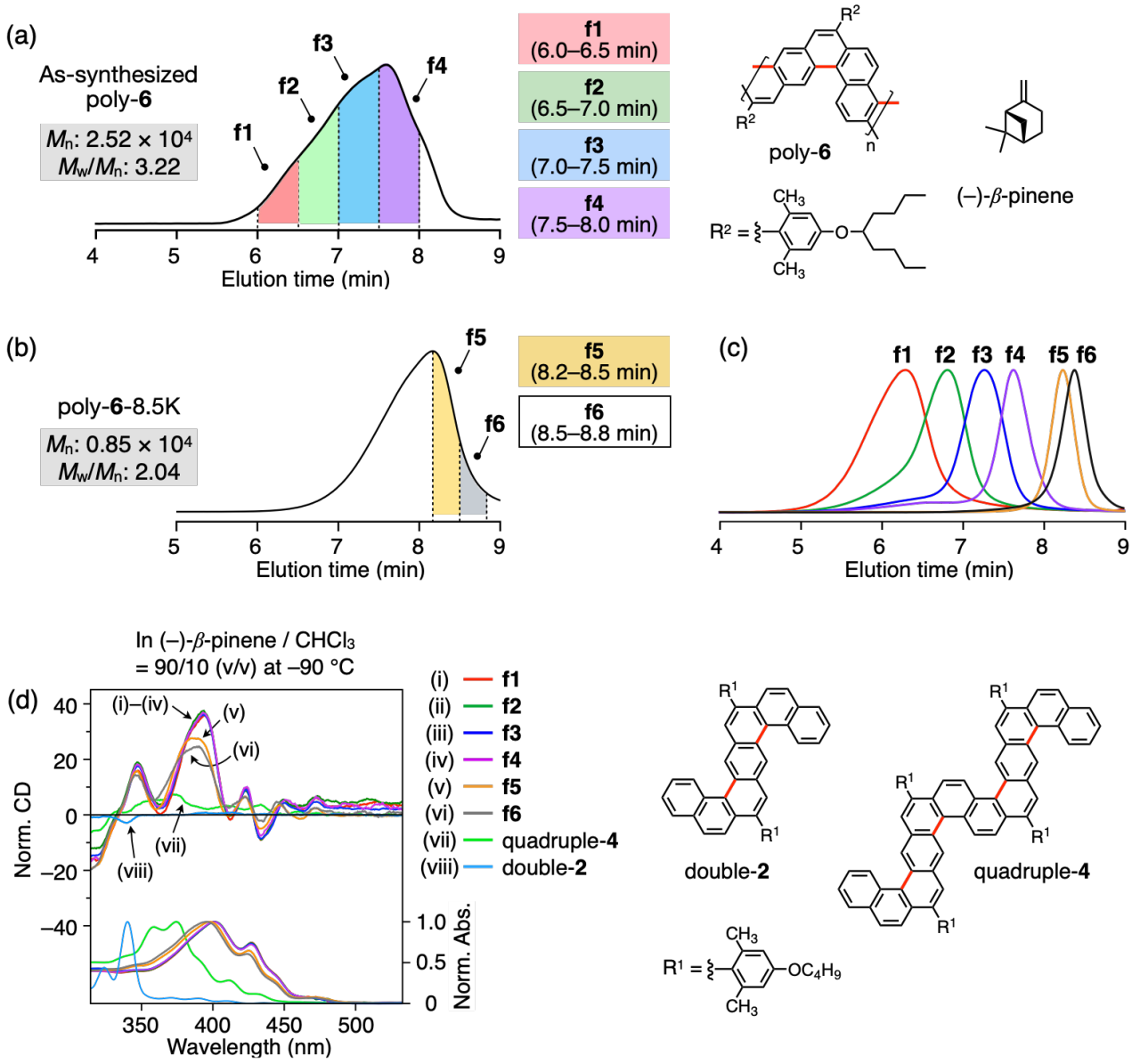

fraction	M_n (10^4)	M_w/M_n	DP_n	$\lvert g_{abs}\rvert$ (10^{-3}) at the maximum Cotton effect
(—,●) **f1**	20.4	1.72	275	1.16 (389 nm)
(—,●) **f2**	8.25	1.68	111	1.22 (389 nm)
(—,●) **f3**	2.99	1.19	40	1.19 (389 nm)
(—,●) **f4**	1.40	1.15	19	1.20 (389 nm)
(—,●) **f5**	0.64	1.10	9	0.94 (382 nm)
(—,●) **f6**	0.48	1.14	6	0.82 (386 nm)
(—,●) quadruple-**4** (MW: 1334)				0.23 (369 nm)
(—,●) double-**2** (MW: 731)				0.09 (338 nm)

Supplementary Fig. 25 | (a–c) SEC traces of as-synthesized poly-**6** (a), poly-**6**-8.5K (b), and their fractionated components (**f1** – **f6**) with different molar masses (c) (eluent, chloroform; polystyrene standards). (d) CD and absorption spectra of fractionated polymers (**f1** – **f6**) measured in (–)-*β*-pinene/chloroform (90/10, v/v) at –90 °C after SEC fractionation. The CD and absorption spectra were normalized based on the corresponding absorption spectra at –90 °C. The corresponding spectra of quadruple-**4** (vii) and double-**2** (viii) measured in (–)-*β*-pinene/chloroform (90/10, v/v) at –90 °C are also shown in (d).

8. Supporting References

S1 Zheng, W., Ikai, T., Oki, K. & Yashima, E. Consecutively-fused single, double, and triple expanded helicenes. *Nat. Sci.* **2**, e20210047 (2022).

S2 Zheng, W., Ikai, T. & Yashima, E. Synthesis of single-handed helical spiro-conjugated ladder polymers through quantitative and chemoselective cyclizations. *Angew. Chem., Int. Ed.* **60**, 11294–11299 (2021).

S3 Xia, J., Golder, M. R., Foster, M. E., Wong, B. M. & Jasti, R. Synthesis, characterization, and computational studies of cycloparaphenylene dimers. *J. Am. Chem. Soc.* **134**, 19709–19715 (2012).

S4 CrysAlisPRO, Oxford Diffraction/Agilent Technologies UK Ltd, Yarnton, England, 2015.

S5 Sheldrick, G. A short history of SHELX. *Acta Crystallogr. Sect. A* **64**, 112–122 (2008).

S6 Sheldrick, G. SHELXT - Integrated space-group and crystal-structure determination. *Acta Crystallogr. Sect. A* **71**, 3–8 (2015).

S7 Sheldrick, G. M. SHELXL-2018/3: Program for the Refinement of Crystal Structures; University of Göttingen, Göttingen, Germany, 2018.

S8 Sheldrick, G. Crystal structure refinement with SHELXL. *Acta Crystallogr. Sect. C-Struct. Chem.* **71**, 3–8 (2015).

S9 Dolomanov, O. V., Bourhis, L. J., Gildea, R. J., Howard, J. A. K. & Puschmann, H. OLEX2: A complete structure solution, refinement and analysis program. *J. Appl. Cryst.* **42**, 339–341 (2009).

S10 Van Der Spoel, D., Lindahl, E., Hess, B., Groenhof, G., Mark, A. E. & Berendsen, H. J. C. GROMACS: Fast, flexible, and free. *J. Comput. Chem.* **26**, 1701–1718 (2005).

S11 Hess, B., Kutzner, C., van der Spoel, D. & Lindahl, E. GROMACS 4: Algorithms for highly efficient, load-balanced, and scalable molecular simulation. *J. Chem. Theory Comput.* **4**, 435–447 (2008).

S12 Abraham, M. J., Murtola, T., Schulz, R., Páll, S., Smith, J. C., Hess, B. & Lindahl, E. GROMACS: High performance molecular simulations through multi-level parallelism from laptops to supercomputers. *SoftwareX* **1-2**, 19–25 (2015).

S13 Becke, A. D. Density-functional exchange-energy approximation with correct asymptotic behavior. *Phys. Rev. A* **38**, 3098–3100 (1988).

S14 Lee, C., Yang, W. & Parr, R. G. Development of the Colle-Salvetti correlation-energy formula into a functional of the electron density. *Phys. Rev. B* **37**, 785–789 (1988).

S15 Becke, A. D. Density‐functional thermochemistry. III. The role of exact exchange. *J. Chem. Phys.* **98**, 5648–5652 (1993).

S16 Gaussian 16, Revision C.01, M. J. Frisch, G. W. Trucks, H. B. Schlegel, G. E. Scuseria, M. A. Robb, J. R. Cheeseman, G. Scalmani, V. Barone, G. A. Petersson, H. Nakatsuji, X. Li, M.

Caricato, A. V. Marenich, J. Bloino, B. G. Janesko, R. Gomperts, B. Mennucci, H. P. Hratchian, J. V. Ortiz, A. F. Izmaylov, J. L. Sonnenberg, D. Williams-Young, F. Ding, F. Lipparini, F. Egidi, J. Goings, B. Peng, A. Petrone, T. Henderson, D. Ranasinghe, V. G. Zakrzewski, J. Gao, N. Rega, G. Zheng, W. Liang, M. Hada, M. Ehara, K. Toyota, R. Fukuda, J. Hasegawa, M. Ishida, T. Nakajima, Y. Honda, O. Kitao, H. Nakai, T. Vreven, K. Throssell, J. A. Montgomery, Jr., J. E. Peralta, F. Ogliaro, M. J. Bearpark, J. J. Heyd, E. N. Brothers, K. N. Kudin, V. N. Staroverov, T. A. Keith, R. Kobayashi, J. Normand, K. Raghavachari, A. P. Rendell, J. C. Burant, S. S. Iyengar, J. Tomasi, M. Cossi, J. M. Millam, M. Klene, C. Adamo, R. Cammi, J. W. Ochterski, R. L. Martin, K. Morokuma, O. Farkas, J. B. Foresman, and D. J. Fox, Gaussian, Inc., Wallingford CT, 2016.

S17 Wang, J., Wang, W., Kollman, P. A. & Case, D. A. Automatic atom type and bond type perception in molecular mechanical calculations. *J. Mol. Graph. Model.* **25**, 247–260 (2006).

S18 Wang, J., Wolf, R. M., Caldwell, J. W., Kollman, P. A. & Case, D. A. Development and testing of a general amber force field. *J. Comput. Chem.* **25**, 1157–1174 (2004).

S19 Sousa da Silva, A. W. & Vranken, W. F. ACPYPE - AnteChamber PYthon Parser interfacE. *BMC Res. Notes* **5**, 367 (2012).

S20 Nosé, S. A molecular dynamics method for simulations in the canonical ensemble. *Mol. Phys.* **52**, 255–268 (1984).

S21 Hoover, W. G. Canonical dynamics: Equilibrium phase-space distributions. *Phys. Rev. A* **31**, 1695–1697 (1985).

S22 Parrinello, M. & Rahman, A. Polymorphic transitions in single crystals: A new molecular dynamics method. *J. Appl. Phys.* **52**, 7182–7190 (1981).

S23 Nosé, S. & Klein, M. L. Constant pressure molecular dynamics for molecular systems. *Mol. Phys.* **50**, 1055–1076 (1983).

S24 Hess, B., Bekker, H., Berendsen, H. J. C. & Fraaije, J. G. E. M. LINCS: A linear constraint solver for molecular simulations. *J. Comput. Chem.* **18**, 1463–1472 (1997).

S25 Darden, T., York, D. & Pedersen, L. Particle mesh Ewald: An N·log(N) method for Ewald sums in large systems. *J. Chem. Phys.* **98**, 10089–10092 (1993).

S26 Ditchfield, R., Hehre, W. J. & Pople, J. A. Self‐consistent molecular‐orbital methods. IX. An extended Gaussian‐type basis for molecular‐orbital studies of organic molecules. *J. Chem. Phys.* **54**, 724‐728 (1971).

S27 Hehre, W. J., Ditchfield, R. & Pople, J. A. Self—consistent molecular orbital methods. XII. Further extensions of Gaussian—type basis sets for use in molecular orbital studies of organic molecules. *J. Chem. Phys.* **56**, 2257–2261 (1972).

S28 Rassolov, V. A., Pople, J. A., Ratner, M. A. & Windus, T. L. 6-31G* basis set for atoms K through Zn. *J. Chem. Phys.* **109**, 1223–1229 (1998).

S29 Gaussian 16, Revision B.01, Frisch, M. J., Trucks, G. W., Schlegel, H. B., Scuseria, G. E., Robb, M. A., Cheeseman, J. R.; Scalmani, G.; Barone, V.; Petersson, G. A.; Nakatsuji, H.; Li, X.; Caricato, M.; Marenich, A. V.; Bloino, J., Janesko, B. G., Gomperts, R., Mennucci, B., Hratchian, H. P., Ortiz, J. V., Izmaylov, A. F., Sonnenberg, J. L., Williams-Young, D., Ding, F., Lipparini, F., Egidi, F., Goings, J., Peng, B., Petrone, A., Henderson, T., Ranasinghe, D., Zakrzewski, V. G., Gao, J., Rega, N., Zheng, G., Liang, W., Hada, M., Ehara, M., Toyota, K., Fukuda, R., Hasegawa, J., Ishida, M., Nakajima, T., Honda, Y., Kitao, O., Nakai, H., Vreven, T., Throssell, K., Montgomery Jr., J. A., Peralta, J. E., Ogliaro, F., Bearpark, M. J., Heyd, J. J., Brothers, E. N., Kudin, K. N., Staroverov, V. N., Keith, T. A., Kobayashi, R., Normand, J., Raghavachari, K., Rendell, A. P., Burant, J. C., Iyengar, S. S., Tomasi, J., Cossi, M., Millam, J. M., Klene, M., Adamo, C., Cammi, R., Ochterski, J. W., Martin, R. L., Morokuma, K., Farkas, O., Foresman, J. B., Fox, D. J. Gaussian, Inc., Wallingford CT, 2016.

S30 Sun, H., Jin, Z., Yang, C., Akkermans, R. L. C., Robertson, S. H., Spenley, N. A., Miller, S. & Todd, S. M. COMPASS II: Extended coverage for polymer and drug-like molecule databases. *J. Mol. Model.* **22**, 47 (2016).

S31 Humphrey, W., Dalke, A. & Schulten, K. VMD: Visual molecular dynamics. *J. Molec. Graphics* **14**, 33–38 (1996).

9. ^{1}H and ^{13}C NMR Spectral Data

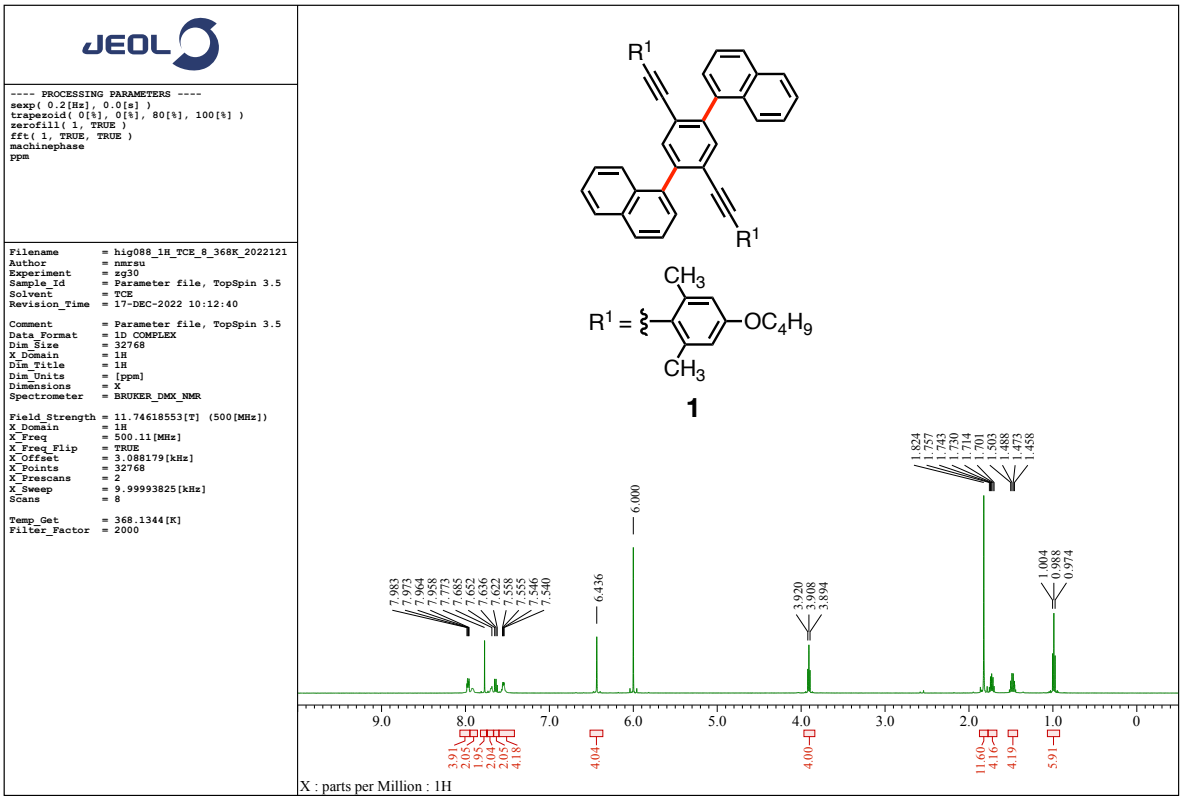

Supplementary Fig. 26 | ^{1}H NMR (500 MHz, 1,1,2,2-tetrachloroethane-d_2, 95 °C) spectrum of **1**.

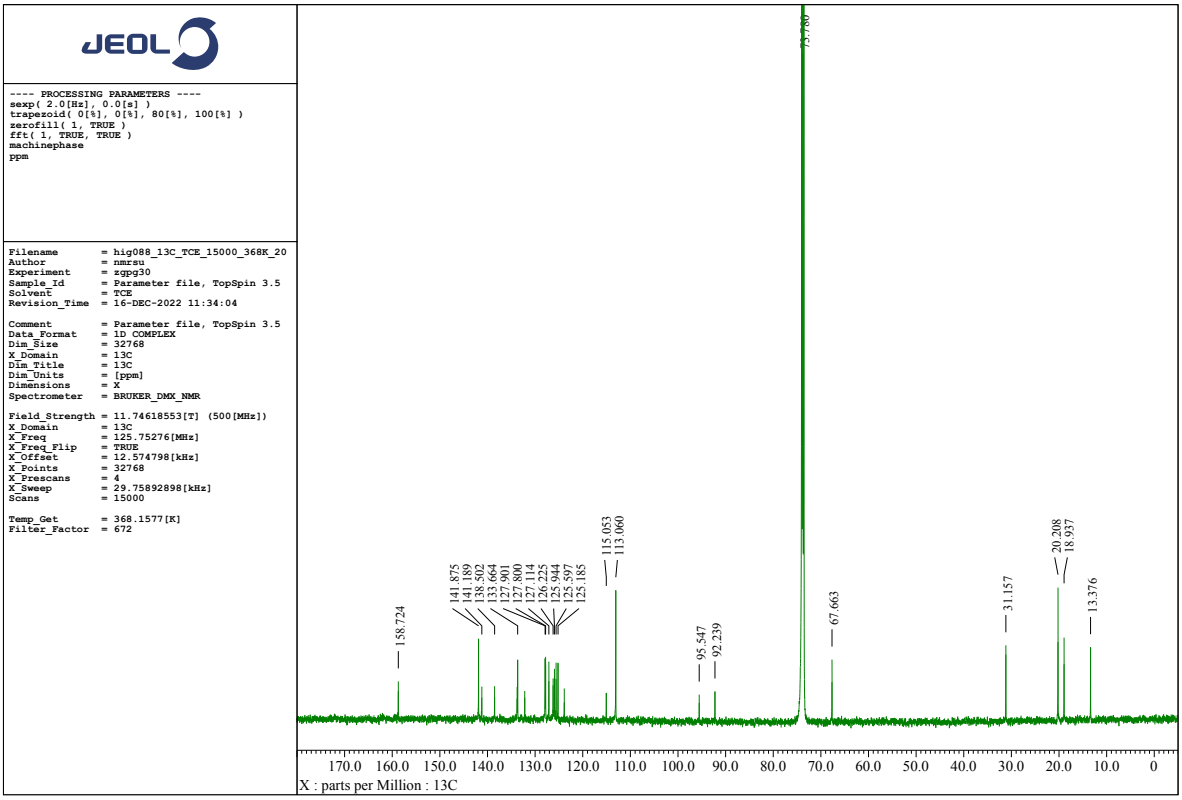

Supplementary Fig. 27 | ^{13}C NMR (126 MHz, 1,1,2,2-tetrachloroethane-d_2, 95 °C) spectrum of **1**.

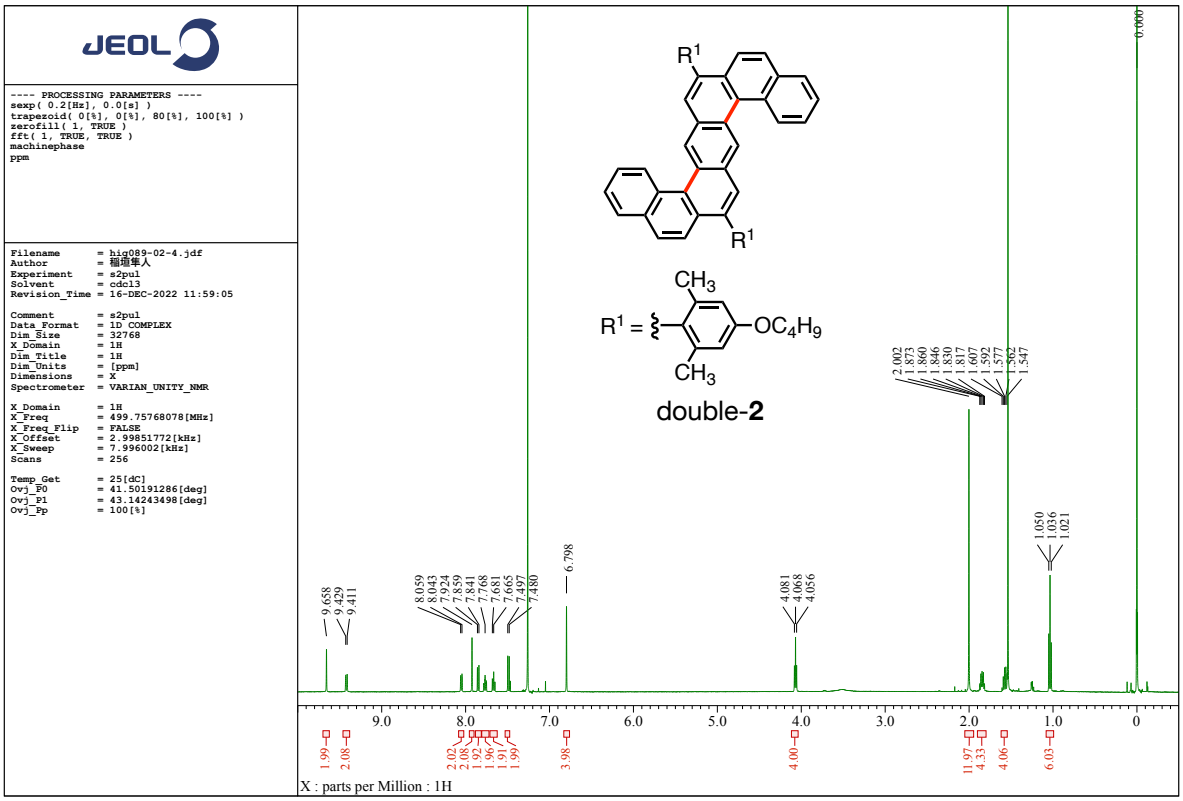

Supplementary Fig. 28 | ^{1}H NMR (500 MHz, $CDCl_3$, 25 °C) spectrum of double-**2**.

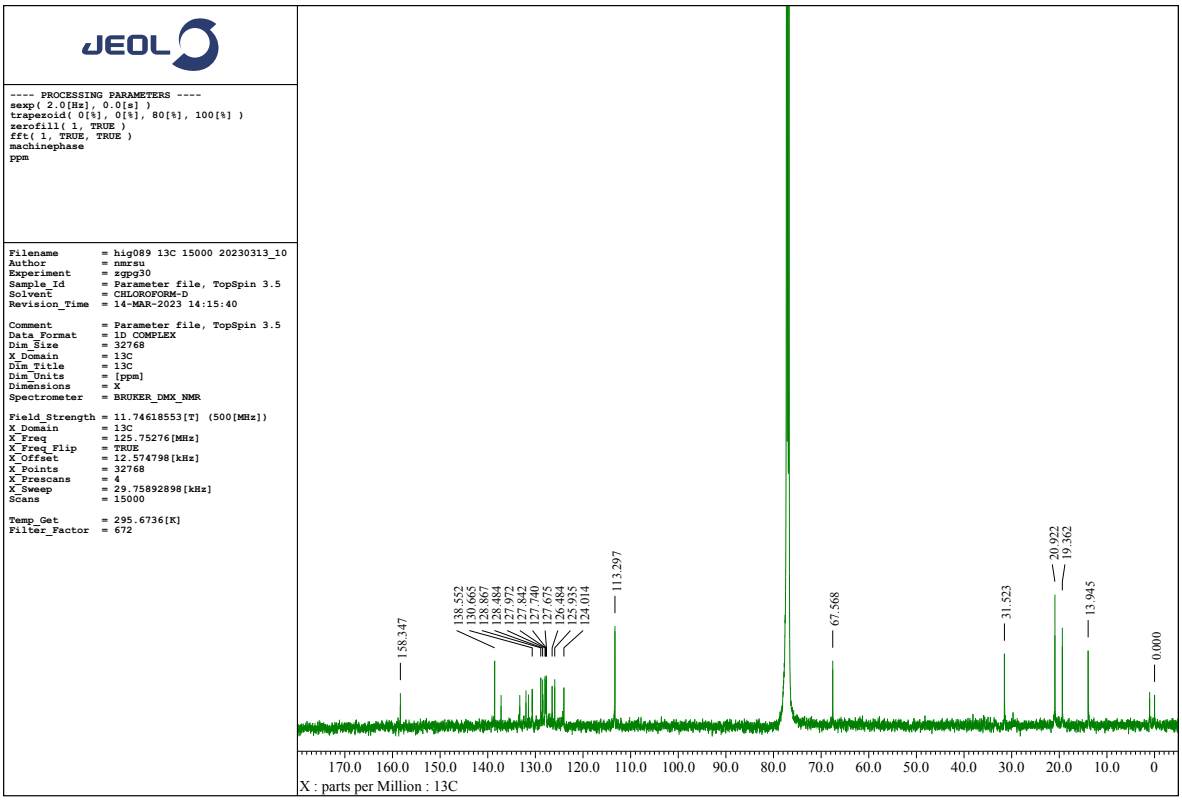

Supplementary Fig. 29 | ^{13}C NMR (126 MHz, $CDCl_3$, rt) spectrum of double-**2**.

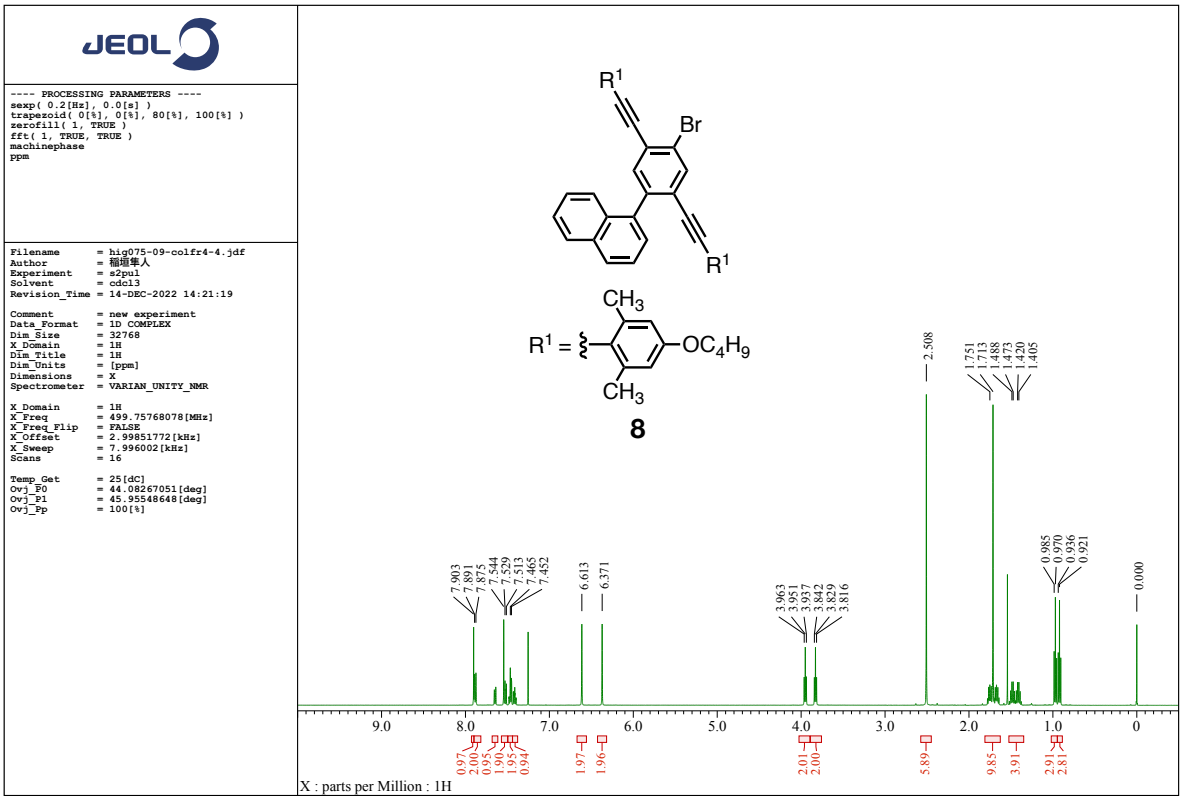

Supplementary Fig. 30 | ^{1}H NMR (500 MHz, $CDCl_3$, 25 °C) spectrum of **8**.

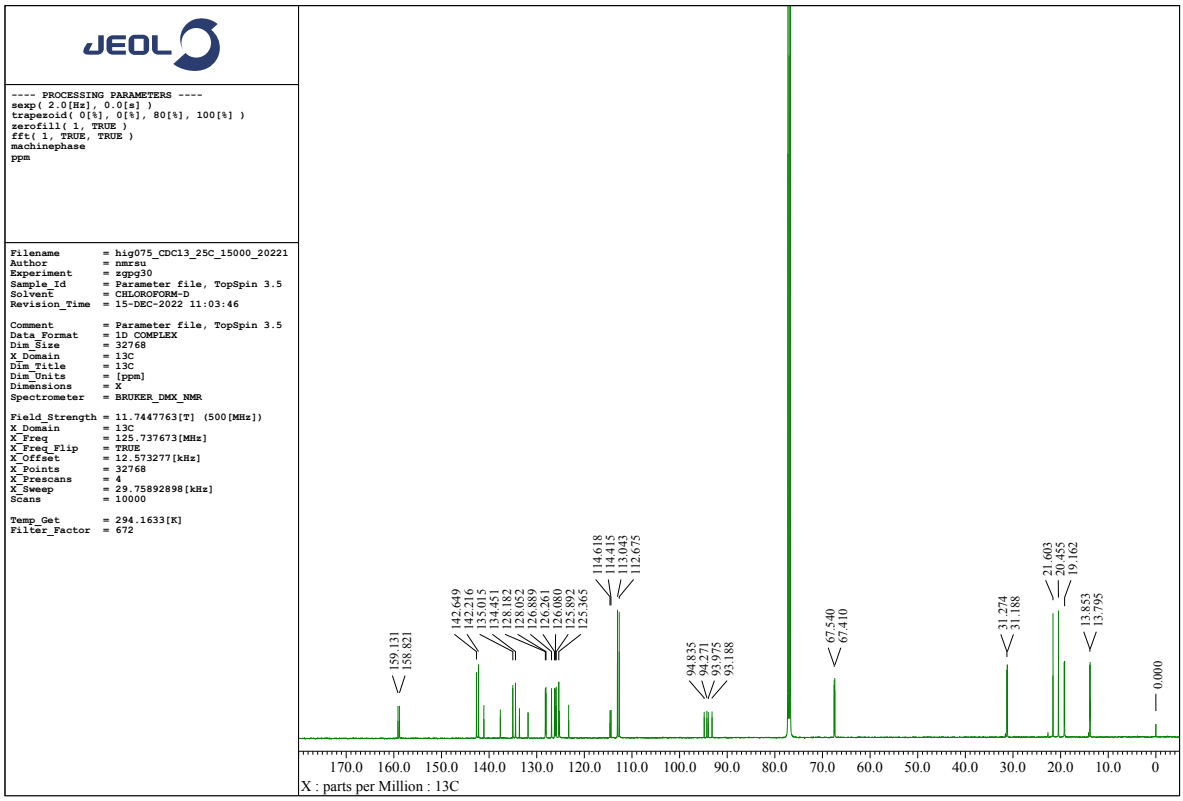

Supplementary Fig. 31 | ^{13}C NMR (126 MHz, $CDCl_3$, rt) spectrum of **8**.

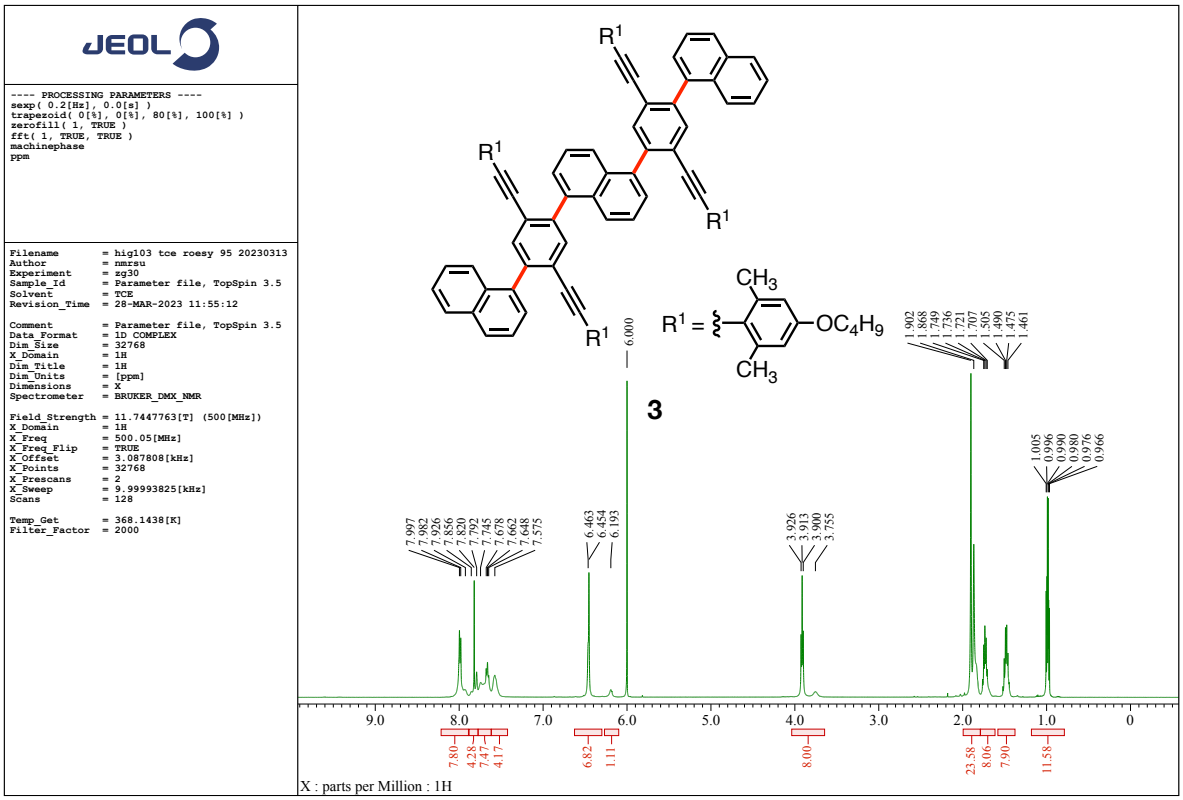

Supplementary Fig. 32 | ^{1}H NMR (500 MHz, 1,1,2,2-tetrachloroethane-d_2, 95 °C) spectrum of **3**.

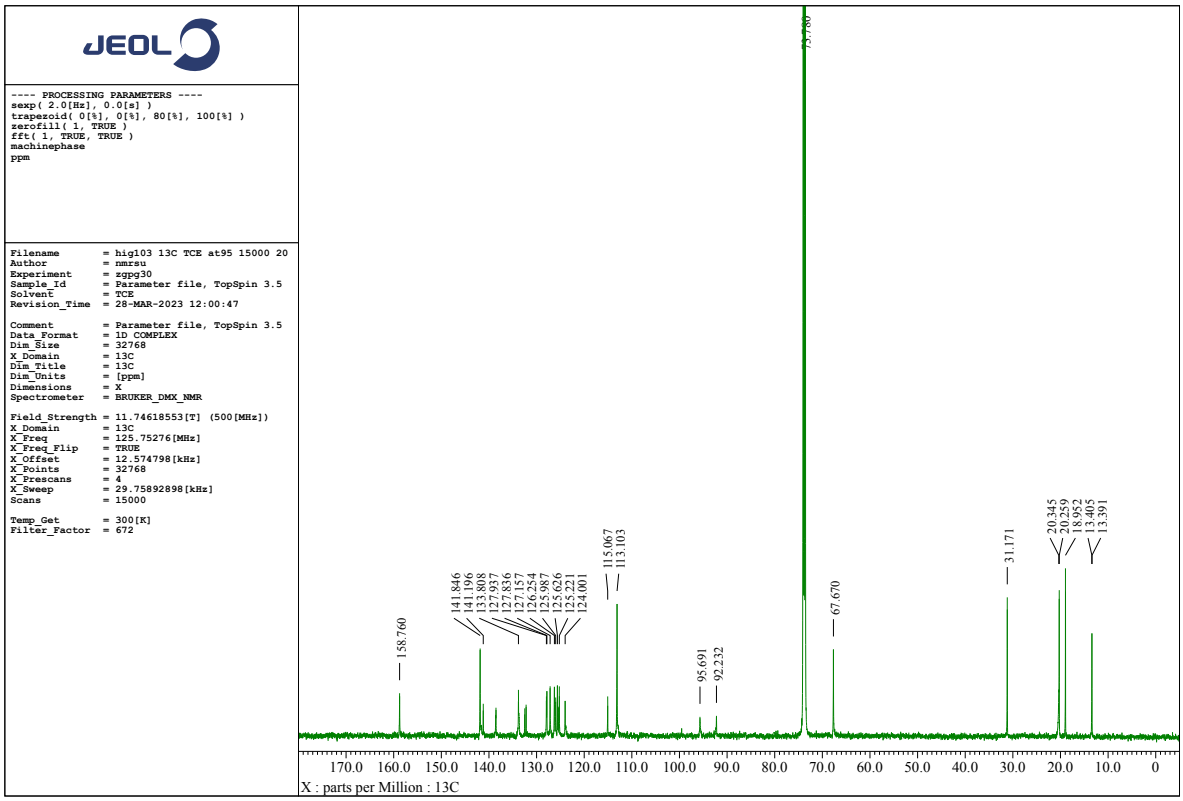

Supplementary Fig. 33 | ^{13}C NMR (126 MHz, 1,1,2,2-tetrachloroethane-d_2, 95 °C) spectrum of **3**.

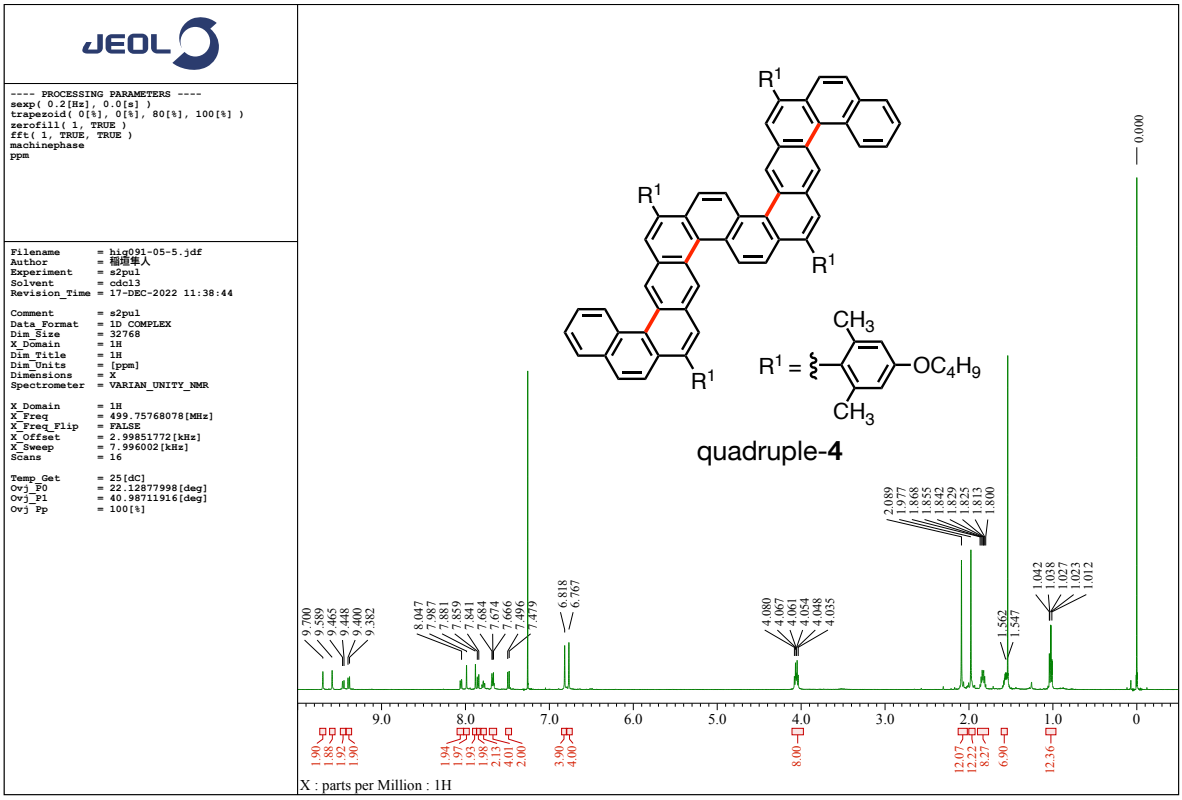

Supplementary Fig. 34 | ^{1}H NMR (500 MHz, $CDCl_3$, 25 °C) spectrum of quadruple-**4**.

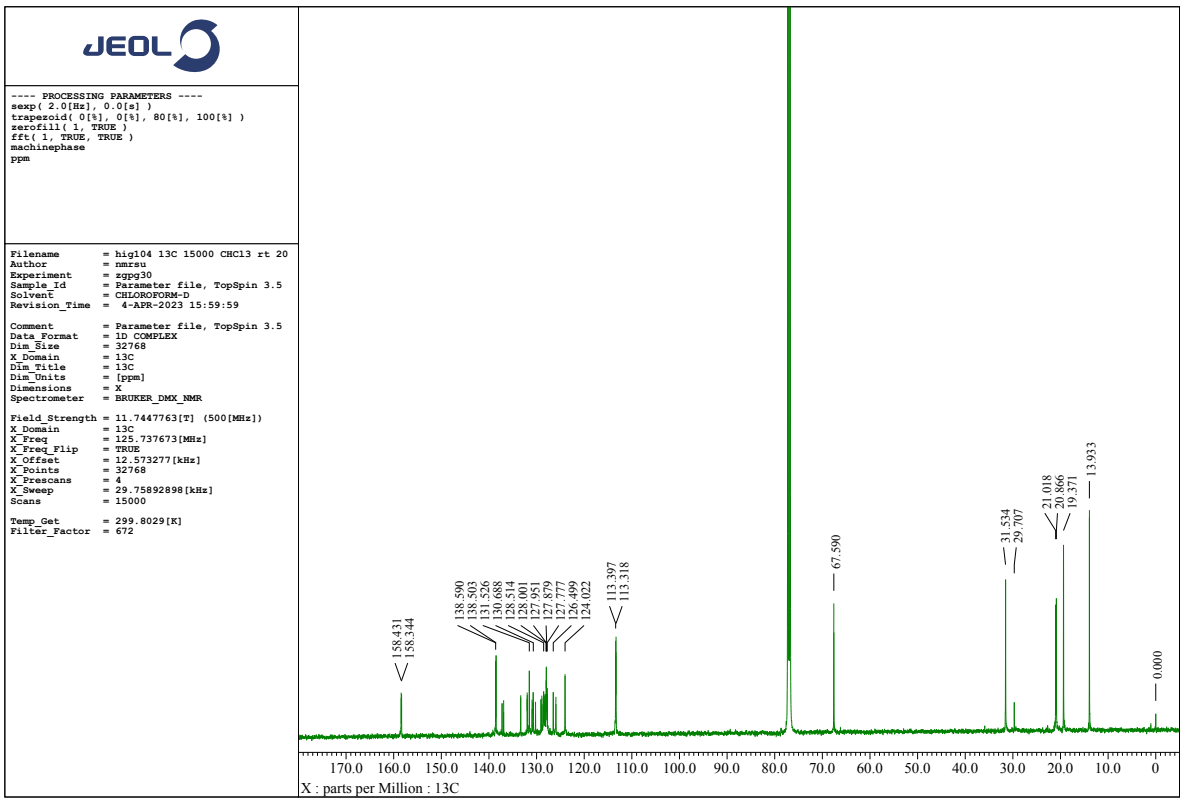

Supplementary Fig. 35 | ^{13}C NMR (126 MHz, $CDCl_3$, rt) spectrum of quadruple-**4**.

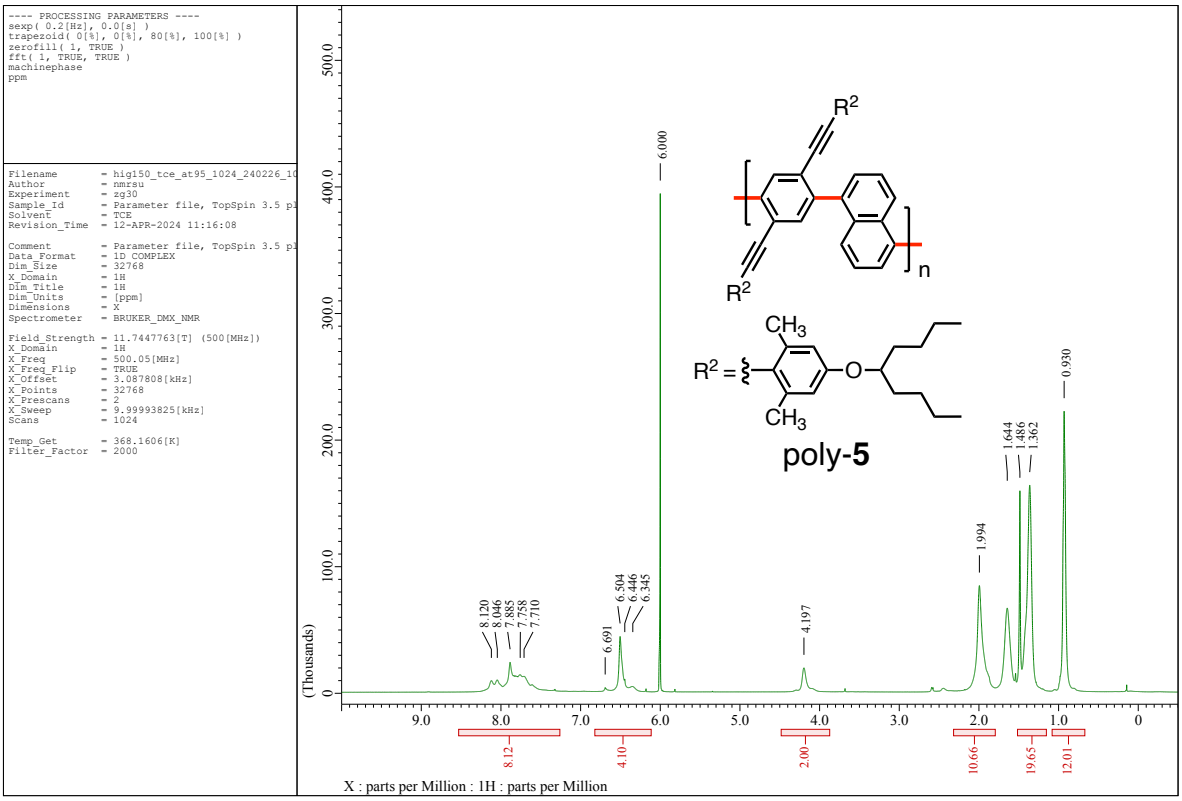

Supplementary Fig. 36 | ^{1}H NMR (500 MHz, 1,1,2,2-tetrachloroethane-d_2, 95 °C) spectrum of poly-**5**.

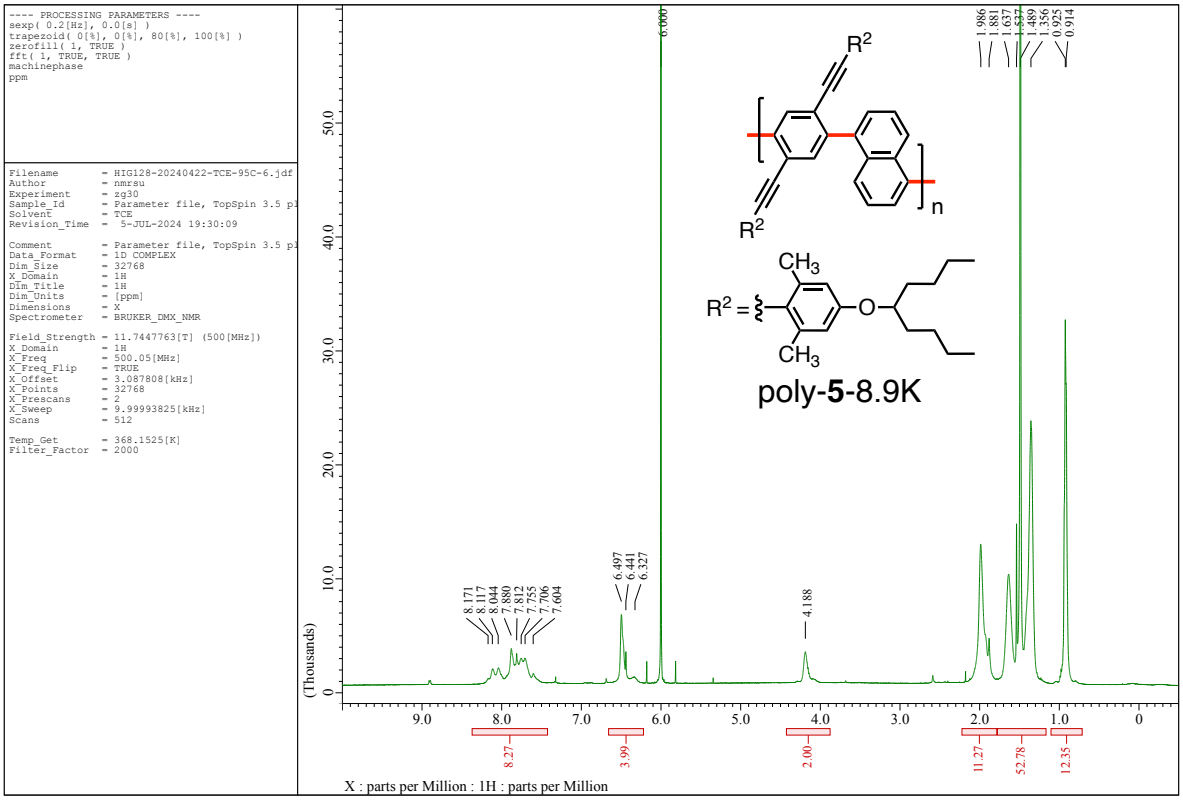

Supplementary Fig. 37 | ^{1}H NMR (500 MHz, 1,1,2,2-tetrachloroethane-d_2, 95 °C) spectrum of poly-**5**-8.9K.

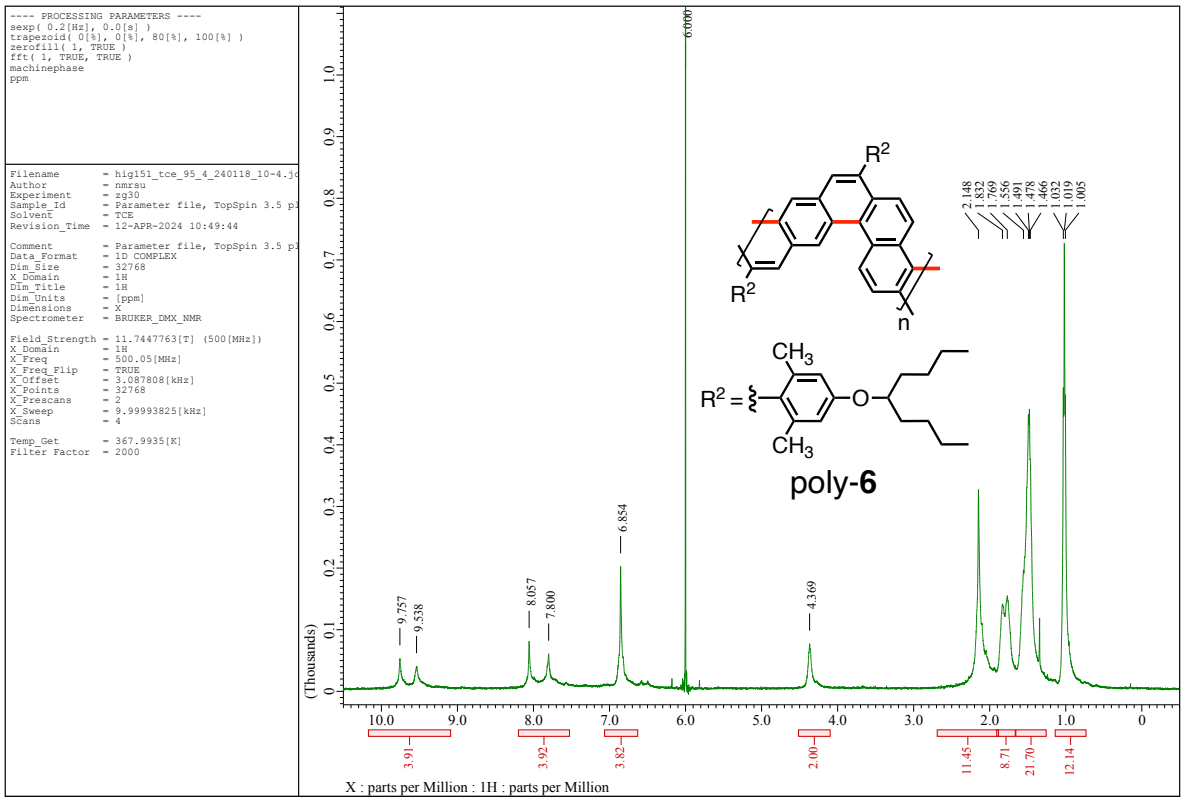

Supplementary Fig. 38 | ^{1}H NMR (500 MHz, 1,1,2,2-tetrachloroethane-d_2, 95 °C) spectrum of poly-**6**.

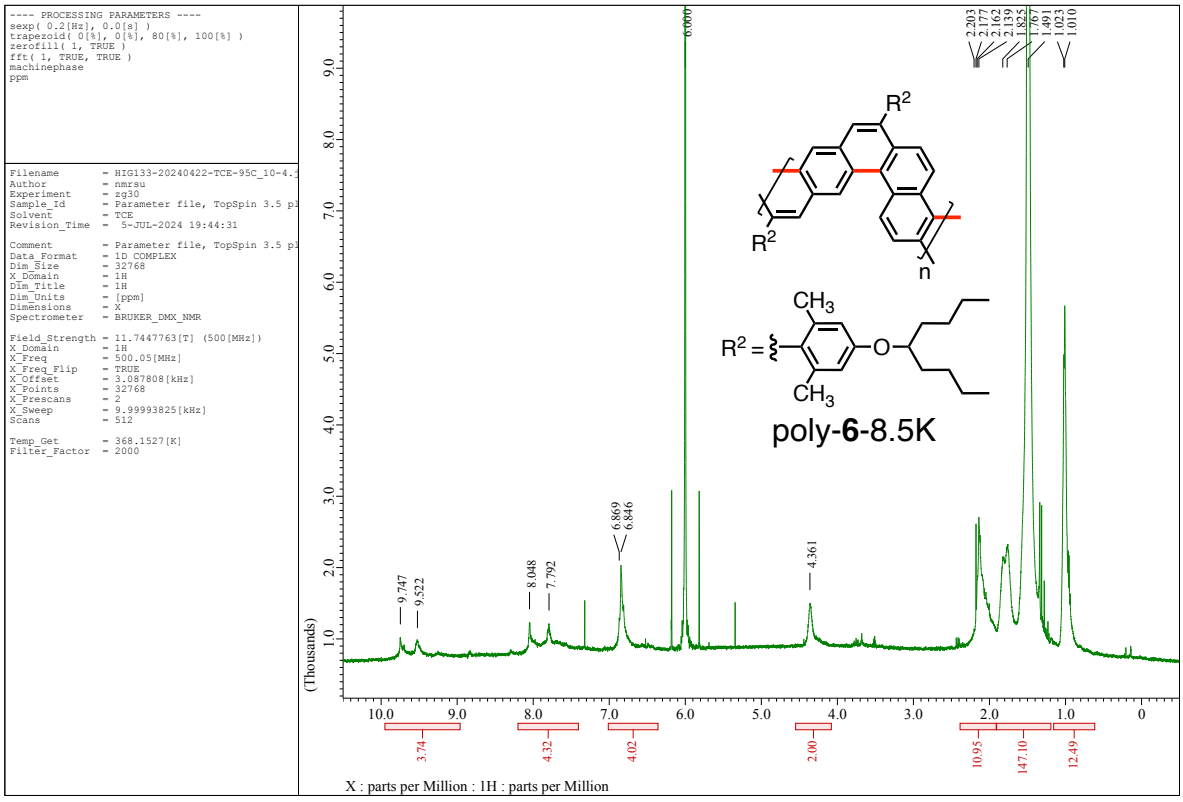

Supplementary Fig. 39 | ^{1}H NMR (500 MHz, 1,1,2,2-tetrachloroethane-d_2, 95 °C) spectrum of poly-**6**-8.5K.

10. Captions for Supporting Videos

Supplementary Video 1. The side view of the [4]helicene-based graphene nanoribbon (poly-**6**) of the 60 ns MD trajectory in the chloroform solvent at 293.15 K. Chloroform is not shown for clarity, and two colors (cyan and blue) are used to make the monomer units clear. The movies were prepared by VMD software.[S31] The animations were smoothed by averaging 5 frames for each frame of the movie to enhance visualization.

Supplementary Video 2. The side view of the [4]helicene-based graphene nanoribbon (poly-**6**) of the 60 ns MD trajectory in the chloroform solvent at 400 K. Chloroform is not shown for clarity, and two colors (cyan and blue) are used to make the monomer units clear. The movies were prepared by VMD software.[S31] The animations were smoothed by averaging 5 frames for each frame of the movie to enhance visualization.